



Norwegian University of
Science and Technology

G2 checkpoint siRNA screen in irradiated cancer cells: validation of candidate positive hits

Ingrid Marie Eriksen Daviknes

Chemical Engineering and Biotechnology

Submission date: July 2011

Supervisor: Per Bruheim, IBT

Co-supervisor: Randi Syljuåsen, Avd. for Strålingsbiologi, Institutt for
Kreftforskning, Radiumhospitalet

Declaration

I hereby declare that the work presented in this thesis is executed in accordance to “Reglement for sivilarkitekt-/sivilingeniøreksamen “at Norwegian University for Science and Technology

Oslo 4.7.2011,

Ingrid Daviknes

Preface

This master's thesis is the final project for receiving the Master of Science degree in Industrial Chemistry and Biotechnology at Norwegian University for Science and Technology (NTNU). It has been carried out at the Department of Radiation Biology, Institute of Cancer Research at the Norwegian Radium Hospital.

First, I would like to thank my supervisor at the Department of Radiation Biology, Randi G. Syljuåsen, for advice, support and encouragement.

I am very thankful to PhD student Viola Nähse-Kumpf for the daily guidance in the laboratory work and for all her good advice. I also want to thank the rest of Randi Syljuåsens' research group for all the help and support.

I would also like to thank my supervisor at NTNU, Per Bruheim.

Oslo, 04.07.2011

Ingrid M. E. Daviknes

Table of Contents

Preface.....	3
Table of Contents	4
Abstract	7
1. Introduction and aims	8
2. Theory.....	11
2.1 The cell cycle.....	11
2.1.1 The normal cell cycle.....	11
2.1.2 Cell cycle phases	11
2.1.3 Abnormal cell cycling (cancer)	15
2.2 The DNA damage-induced cell cycle checkpoints	16
2.2.1 DNA damage signaling	17
2.2.2 Cell cycle checkpoints	19
2.3 G2-checkpoint and cancer relevance	23
2.3.1 Loss of Checkpoint, Genomic instability and Cancer development	23
2.3.2 Limitation of checkpoints can contribute to genetic instability.	24
2.3.3 Principles of cancer treatment.....	25
2.3.4 G2 checkpoint as a therapeutic target.....	25
2.3.5 WEE1-inhibitor	26
2.3.6 CHK1- inhibition or silencing.....	26
2.4 mRNA silencing.....	27
2.4.1 SiRNAs	27
2.4.2 EsiRNAs.....	29
3. Materials, chemicals and instruments	30

4. Methods	37
4.1 Cell cultivation	37
4.2 Effectene esiRNA transfection.....	38
4.3 Oligofectamine siRNA transfection	40
4.4 WEE1 inhibition	40
4.5 IR	41
4.6 Early versus Late G2 Checkpoint	41
4.7 Harvesting and Fixing.....	42
4.8 a) Immunostaining for Flow Cytometry.....	43
4.8 b) Flow cytometry analysis	44
4.9 Immunostaining of Coverslips for Immunofluorescence microscopy.....	45
4.10 Prior to cell lysates preparation	46
4.11 Cell lysate preparation.....	46
4.12 Protein Quantification	47
4.13 Gel electrophoresis, Western Blotting and immunodetection	48
5. Results.....	50
5.1 Visualization of IR induced DNA damage in U2OS cells	50
5.2 Wee1 inhibition	53
5.2.1 Phenotypic analysis.....	53
5.2.2 Comparison of WEE1 inhibition in early- and late G2 checkpoint in U2OS cells.....	54
5.2.3 U2OS cells versus U2OSp53dd cells: Early G2 checkpoint.....	55
5.3. Validation of hits from phosphatome screen:.....	56
5.3.2 Optimization of transfection reagents: Oligofectamine compared to Effectene.....	58
5.3.3 Optimization of effectene as a transfection reagent for esiRNAs.....	59
5.3.4 Preliminary results on validation of phosphatome-screen hits.....	61
6. Discussion	62
6.1 Confirming the siRNA assay.....	62

6.1.1 WEE1 inhibition.....	62
6.1.2 Current research for WEE1 inhibition.....	63
6.1.3 Future goals for G2/M checkpoint abrogation studies.....	64
6.2 Validation of hits from the siRNA screen	65
6.2.1 EsiRNA transfection	65
6.2.2 Optimization of esiRNA transfection	65
6.2.3 Validation experiments of esiSSH3 and PTPN7	67
6.2.4 Comparison to other G2 checkpoint siRNA screens	67
6.2.5 Future work.....	68
7. Conclusion	69
8. References	70

Appendix A: Hits from the phosphatome- siRNA screen

Appendix B: Raw- and normalized data (MI) from flow cytometry analysis

Abstract

Prior to this project, a high throughput assay was developed in order to perform automated RNAi screens with siRNA- libraries targeting potential regulators of the G2 checkpoint. The libraries were covering the human kinases, phosphatases and DNA repair. The aim of this project was to validate the candidate hits from the phosphatome screen as possible G2 checkpoint regulators. To validate the candidate hits, esiRNAs were applied in order to down regulate the target proteins, and G2 checkpoint abrogation was assayed by flow cytometry analysis. To confirm that the assay did work, the effects of inhibiting WEE1 by the small molecule inhibitor, MK1775, were tested in both U2OS and U2OSp53 cells. Both the early and the late G2 checkpoint were tested for.

WEE1 was a hit in the kinome screen, and a well-known regulator of the G2 checkpoint. The samples treated with MK1775, and 6Gy were showing a dose-dependent abrogation of the G2 checkpoint when stained for H3-p and analyzed by flow cytometry.

In optimization experiments for esiRNA transfection, Effectene was chosen over Oligofectamine as the preferred transfection reagent. The transfection conditions which were decided to be the most efficient in down regulating the target protein were 5µL esiRNA and 10 µL Effectene. For the validation experiments it was focused on the two phosphatases SSH3 and PTPN7. Western blotting analysis showed that the protein level of SSH3 was reduced to less than 50% at two days following transfection with SSH3 esiRNA.

The validation experiment did not show any abrogation of the G2 checkpoint by neither SSH3 nor PTPN7 in irradiated cells. More repetitions of the experiment are needed in order to validate- or reject these as false hits. However, the results from a whole-genome DNA damage response siRNA screen were recently published. Neither PTPN7 nor SSH3 were scoring in this screen. These facts are supporting the results that SSH3 and PTPN7 are false hits.

1. Introduction and aims

DNA damaging agents such as ionizing irradiation are frequently used for anti-cancer therapy. Obstacles that are encountered are such as tumor radio resistance and IR induced damage to non-tumor cells. An ideal approach would be an agent which causes radio resistance in tumor cells, but spares the normal tissue.

The cells exhibit mechanisms to discover DNA damage, to arrest damaged cells from cycling and to initiate proper DNA repair and/or apoptosis. These mechanisms are controlled by the cell cycle DNA damage checkpoints, denoted G1-, S- and G2 phase checkpoints. The downstream signaling pathways activated by DNA damage are currently of interest in cancer treatment research. The S-phase checkpoint is rather slowing down, than arresting the cells. In many cancers, the tumor suppressor gene, P53, is mutated or contains deletions, resulting in a deficient G1 DNA damage checkpoint[1]. Consequently, these tumor cells are only dependent on the G2 checkpoint. The G2 checkpoint has a critical role in cancer cells, and thus been named *“The key guardian of the cancer cell genome”*[1]. This makes the phosphatases and kinases that control the G2 checkpoint a target for cancer therapy. Abrogation of the G2 checkpoint of DNA damaged cancer cells will induce a premature mitotic entry leading to apoptosis and mitotic catastrophe, a special form for cell death[2].

Prior to this project, a high throughput assay was developed in order to perform automated RNAi screens with siRNA- libraries targeting potential regulators of the G2 checkpoint. The libraries were covering the human kinases, phosphatases and DNA repair factors[3]. The screens were performed by *Viola Nähse-Kumpf Christin Lund-Andersen and Randi G Syljuåsen* at the Department of Radiation Biology, Radiumhospitalet, in collaboration with researchers at BRIC Biocenter at Copenhagen University. Among the hits were several known G2 checkpoint regulators, but also about 50 unknown regulators.

The phosphatome screen, which is the background for this thesis, was performed with an *Ambion* siRNA-library targeting the human phosphatome. Three individual plated siRNAs were employed per target, and transfected reversely in 384-well plates with plated U2OS

(osteosarcoma) p53 deficient cells. The transfected cells were irradiated with 6Gy 2 days later for the induction of G2/M checkpoint. Nocodazole, an inhibitor of development of the mitotic spindle was added subsequently 2 hours post IR, and cells were incubated for 8 hours. The principle of histone H3 phosphorylation in mitotic cells is used to quantify the fraction of cells escaping the G2 checkpoint[3].

The fraction of H3Ser10p-positive cells was stained with H3Ser10p-antibody, and an automated microscope image acquisition was applied for detection of this fraction. The results were analyzed statistically to identify the hits, by making the measurements between the plates comparable[4]. In the phosphatome screen, the threshold for characterizing a hit was set to about 1% H3-p positive cells per sample. The hits from the phosphatome siRNA screen performed prior to this project are presented in **table A1** in **appendix A[3]**.

The aim of this project is to validate candidate positive hits obtained in the G2 checkpoint phosphatome siRNA screen. Several different oligos (siRNAs) must down regulate a target protein subsequently abrogating the G2 checkpoint in order to validate a candidate as a hit. One explanation for the G2-checkpoint abrogation by single siRNAs in the original screen could be off target effects. To exclude that the effects are due to off target effects, esiRNAs are used to down regulate the candidate hits that scored with a single siRNA in the original screen. EsiRNAs are known to cause less off-target effects than siRNAs. First, the G2 checkpoint abrogation assay has to be tested. WEE1, one of the hits from the kinome screen is a known regulator of the G2 checkpoint, and is found to be overexpressed in several types of cancer such as osteosarcoma[1]. The first goal is to control that WEE1 depletion with a small molecule WEE1 inhibitor, MK1775, is leading to G2 checkpoint abrogation. Inhibition with WEE1 in both early and late G2 checkpoint in U2OS cells, and then in U2OSp53dd cells is investigated.

The cells are first treated with WEE1inhibitor, MK1775, and subsequently irradiated with 6Gy 15 minutes later. For the early G2 checkpoint experiments, cells are fixed 90 minutes post-IR. In contrast, for the late G2 checkpoint experiments, nocodazole is added 2 hours post-IR, and cells are fixed 8hours later.

For both early-and late checkpoint the cells are subsequently stained with H3Ser10p antibody to stain mitotic cells, γ -H2AX to localize the Double Stranded Breaks and Hoechst to stain the nuclei. Then the phenotype is analyzed by flow cytometry.

When this is confirmed, some of the hits from the phosphatome screen can be tested for by transfection of the proper esiRNA. EsiRNAs have less off-target effects than siRNAs. U2OS (U2OS p53dneg) cells are transfected and, after incubation for 48, or 72-hours, treated with 6 Gy of IR. Subsequently, cells are treated with nocodazole 2 hours later, and incubated for 8 h. Further, the cells are stained with H3Ser10p antibody to stain mitotic cells, γ -H2AX to localize the Double Stranded Breaks and Hoechst to stain the nuclei. Then the phenotype is analyzed by flow cytometry.

Protein levels in transfected and irradiated cells are controlled by Western Blotting staining for the desired protein

If a candidate hit can be down regulated by several oligos (siRNAs and esiRNAs), and abrogating the G2 checkpoint at the same time, then the candidate is validated as a hit.

The long-term goal is to discover the exact molecular mechanisms of the validated hits, and how these regulators are involved in the G2 checkpoint control after IR.

2. Theory

2.1 The cell cycle

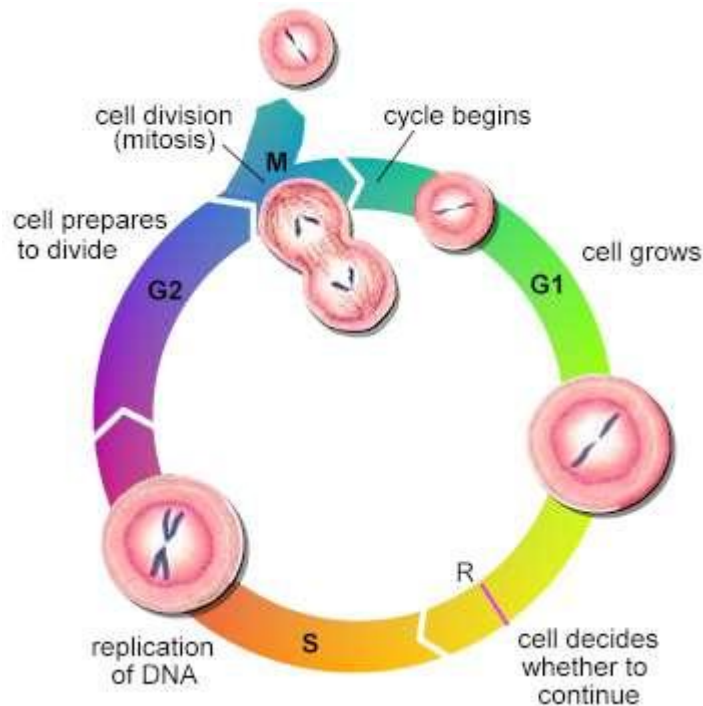


Figure 2.1.: Cell cycle phases. The illustration above is describing the mitotic cell cycle and its major events[2]

2.1.1 The normal cell cycle

All living cells undergo division in order to reproduce, and to yield two or more distinct daughter cells. The number of divisions varies from cell type to cell type. *Mitotic* cells yield only two daughter cells per cycle, by division of the cell after doubling its DNA contents. The division of a cell, its DNA and the events prior to, are defined as the *cell cycle*[3]. The cell cycle and its major events are shown in **figure 2.1.**

2.1.2 Cell cycle phases

The series of stages necessary for division are divided into two major events: *Interphase* and *Mitosis*. Interphase includes all the preparatory phases for division and the mitosis/ where segregation and nuclear division occur. Human cells ingrown in a culture have typically a cycling time of 24 hours, and 95% of this time is spent in interphase[5]. The cell cycle-phases and the most important molecules are shown in **figure 2.2.**

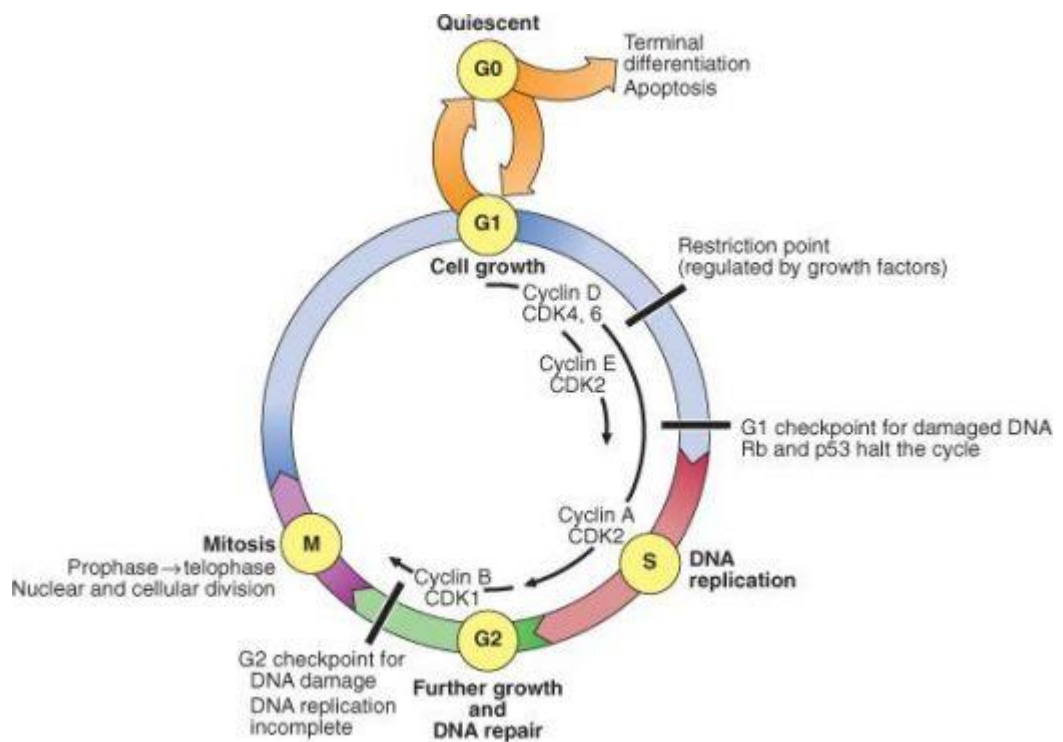


Figure 2.2 : The mitotic cell cycle; its phases, restriction points and driving forces in form of regulatory proteins and kinases (cyclin-CDKs) are shown above[5]

G0 cells may either be terminally differentiated cells, for example nerve cells, or cells capable of dividing. They are nonproliferating due to lack of access to nutrients or growth factors. In the second case, the cells would be able to re-enter the cell cycle to G1 phase if they re-gain access to the nutrients or growth factors.

G1 phase is mainly the phase in between of mitosis and S phase, and is characterized by metabolic growth by transcription and translation of respectively RNA and proteins needed for growth. G1 can shortly be described as a phase where cells undergo maturation to accomplish their physiologic function [6]. The amount of DNA remains constant and condensed. When the cell reaches a certain size, *S-phase* is induced, and DNA-replication can occur [7-9]. Some of the cells in G1 phase that fail to progress to S-phase, exit from the cell cycle, and enters the G0 phase [6].

DNA replication is influenced by several factors; nutrients, mitogens, cytostatic factors and the extracellular matrix[10].

The progression through the cell cycle and the different phases is driven by *cyclins* and Cyclin Dependent Kinases, *CDKs*. Cyclins are key regulators of the cell cycle progression, by binding and activating CDKs. The concentration of cyclins varies throughout the cell cycle, and the CDK activity during different stages of the cell cycle is shown in **figure 2.3**. When the cyclin-CDK complex reaches a threshold level, a transition from one phase to another is initiated.

Induction of S-phase is due to temporary over expression of G1-phase cyclin D and E which in turn activates G1-CDKs; CDK4,CDK6. The cyclin-CDK complex works to phosphorylate and inactivate the retinoblastoma (Rb) tumor suppressor protein. This action allows accumulation of transcription-activity of Elongation Factor 2 protein (E2F) [3, 7, 11]. E2F is a transcription factor, and its targets are transcription of genes encoding DNA replication proteins. G1/S-phase transition also starts the degradation of G1 phase cyclin. S-phase is induced by increasing activity of cyclinA –CDK2, also called the S-phase Promoting Factor (SPF). S-phase is often denoted as *Synthesis Phase* due to the synthesis of new DNA and duplication of the chromatids during the phase. The DNA is doubled in order to allow division of the genetic material into the daughter cell .The cell is dependent on faithful duplication of its genetic material, and several mechanisms are controlling this by detecting and repairing DNA damage from exogenous factors or replication errors. [12].

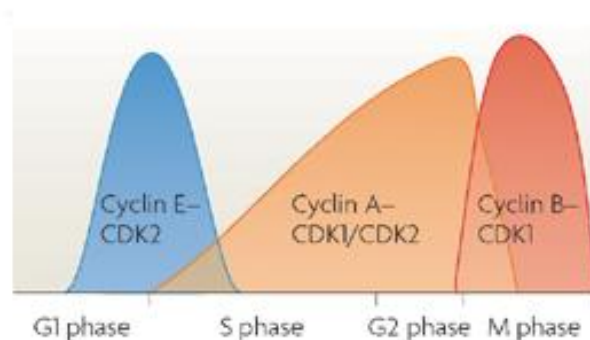


Figure2.3: Cyclin-CDK activity. The figure is showing varying cyclin-CDK complex activity during the cell-cycle[13].

When DNA replication of the chromosomes has successfully completed in S-phase, the cell is ready to move into *G2 phase*. In the *G2 phase* the cell continues to grow rapidly, and synthesizes proteins necessary for cell division in *mitosis* (M phase). As shown in

figure 2.3, the activity of Cyclin A-CDK complexes continues to increase during G2 phase. At the transition to M phase it is rapidly degraded, at the same time as cyclin B levels are accumulating in the cytoplasm and binding to CDK1. Once the activity of cyclinB-CDK1 complex reaches the threshold value, the transition from G2 to mitosis is initiated. The cyclin B-CDK1 is consequently called The Mitosis Promoting Factor (MPF) –complex.[13]

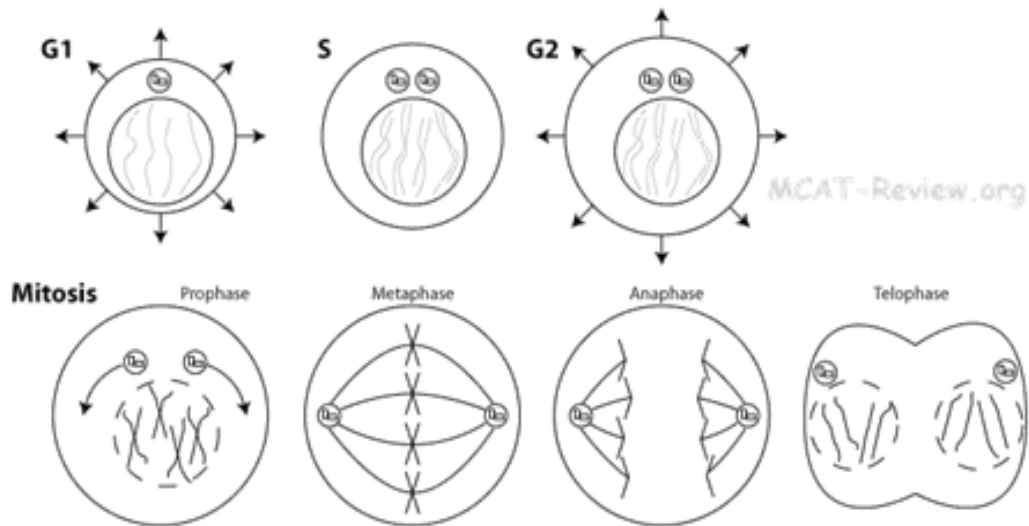


Figure2.4: Characteristics of cell cycle phases. A detailed illustrations of characteristics defining the different phases- and sub- phases during the cell cycle are shown above [14].

When a cell enters mitosis, it enters the Prophase which is the first stage of subdivisions in mitosis. The mitosis can be subdivided into Prophase, Metaphase, Anaphase and Telophase. The organization of DNA in the different phases throughout the cycle is shown in **figure 2.4**. In prophase, the chromatin structure condenses into chromosomes, and the nuclear envelope breaks down. Assembly of the mitotic spindle occurs, and then the centriole pairs are polarized at opposite poles in the cell. In Metaphase, the chromosomes lines up at the “equatorial plate” equidistant from the two poles. Entry into Anaphase does not occur until the chromosomes are properly aligned, which secures symmetric segregation of the sister chromatids. The microtubules are elongated, and the sister chromatids are pulled further apart. In Telophase, the chromatin structure is decondensed and the nuclear envelope reforms, as the mitotic spindle breaks down[14].

While the mitosis divides the nucleus, the Cytokinesis is a separate process dividing the cytoplasm and distributes the organelles to the two daughter cells.

2.1. 3 Abnormal cell cycling (cancer)

A characteristic of cancer cells is their unlimited growth capacity due to loss in control of cell growth. Abnormal cell cycling patterns leading to cancer, is in most cases a result of multiple genetic mutations; either inherited by germ lines or mutations in somatic cells. In most cancers, tumor formation is due to mutation and proliferation of one single tumor cell. The mutation gives this cell an advantage in proliferation and in escaping cell death, which over time gives rise to new mutations and tumor formation. There are two classes of genes involved in cancer; *oncogenes* and *tumor suppressor genes*. [15]

Proto-oncogenes are genes which in their normal form stimulate cell proliferation and growth, but in their mutated forms they are called oncogenes. Proto-oncogene classes include growth factors (often Myc and Bcl-2), growth factor receptors (often tyrosine kinase coupled receptors) and cyclins, and in a mutated form these can stimulate uncontrolled cell division. There are several mechanisms to explain the transition from a proto-oncogene to an oncogene. The first is the occurrence of a point mutation in a proto oncogene. Second, there is gene amplification of a DNA segment containing a proto oncogene leading to over expression of the protein encoded or chromosomal. And third, translocation which alters the expression pattern in a growth-regulatory gene [16].

The second group, tumor-suppressor genes contains genes that prevents cell-division or promote apoptosis. The proteins produced by these genes include; intracellular proteins, hormone-receptors, checkpoint control proteins, apoptosis promoting proteins and repairing proteins [16].

The intracellular proteins are controlling the cell cycle by for example inhibiting cyclin-kinase activity. The hormone receptors are working inhibitory on cell division. Checkpoint controls, explained in detail under **section 2.2.2**, are working to halt cells with DNA damage or chromosomal abnormalities in order to prevent them from undergo division. Repair proteins are activated in presence of DNA damage and checkpoint arrest. In the case of IR- induced double stranded breaks in the DNA, Homologous Recombination (HR) and Non-homologous End Joining (NHEJ) are the cells' strategy for repair. HR is repairing broken DNA ends by exploiting a homologue gene, often in the sister chromatid, leaving very few errors. Initiation of HR starts with resectioning of the DSB to reveal a 3' single

stranded overhang, followed by strand invasion and DNA synthesis of the invading end[17-19].

In contrast to HR, NHEJ is not dependent of a homologous sequence for repair. NHEJ is often considered as a quick and dirty process, meaning that the process is much quicker than HR, but it is more error prone, leaving small deletions or insertions. The DNA ends are religated without a homologous strand [19-21].

The choice between the two DSB repair mechanisms is mostly determined by the cell cycle phases. The HR mechanism is to a great extent restricted to S- and G2 phase when the DNA is decondensed and the sister chromatid is easier available. NHEJ is available in all phases, but are dominating in G1 phase. If the DNA-damage cannot be repaired, programmed cell death is promoted by the last class of tumor-suppressing proteins; apoptosis promoting proteins. Examples on this type of proteins are; p53, p16, Rb, APC and Bax[22].

2.2 The DNA damage-induced cell cycle checkpoints

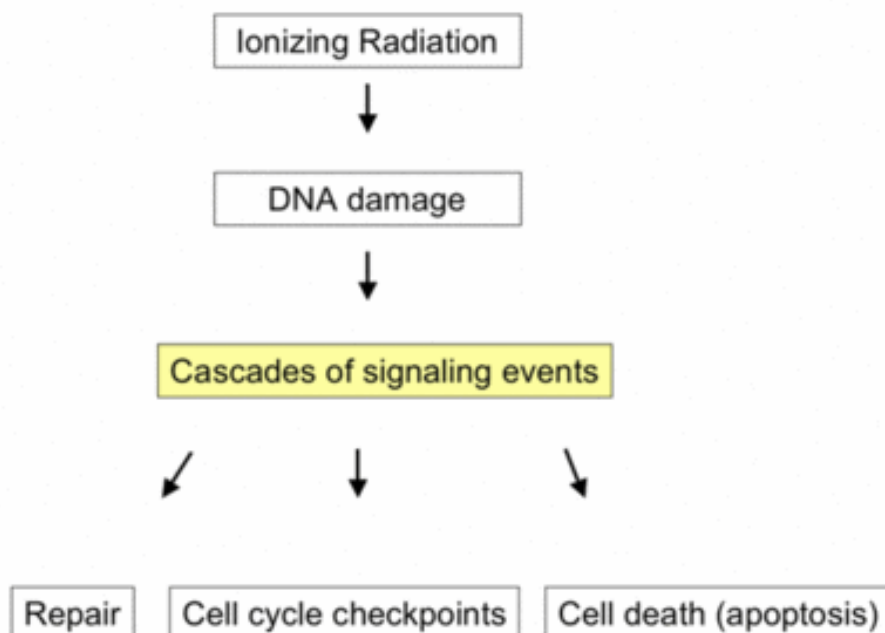


Figure 2.5: IR induced damage. An illustration of the outlines of the downstream processes after IR induced DNA damage is showed above[23, 24]

2.2.1 DNA damage signaling

DNA damage is caused by multiple sources; from ultra violet light (UV) exposure, Ionizing radiation (IR), chemical exposure, cellular metabolism or by replication errors. DNA damage repair is essential for conserving the integrity of the genome. Deficient repair of DNA damage can result in serious consequences such as blockage of transcription and replication, mutagenesis or cytotoxicity. To cope with DNA damage, eukaryotic cells have developed mechanisms to detect DNA damage, to arrest the cell from replicating or dividing with DNA damage and to initiate downstream processes required to maintain genome integrity. These processes are called cell cycle checkpoints, DNA damage repair, apoptosis and/or chromatin remodeling[25].

The main events of IR induced damage response are shown in **figure 2.5**. Ataxia-Telangiectasia mutated (ATM) and ATM and Rad3 Related (ATR) are transducers that recognize DNA damage and are involved in initiation, amplification and activation of cell cycle checkpoints. These checkpoints are the DNA damage checkpoints described below under **section 2.2.2** and denoted G1/S-, S- and G2/M- checkpoints. The DNA damage checkpoints are controlling the status of the cell before critical events in the cell cycle take place, The critical events are prior to initiation of DNA replication, control of newly replicated DNA and before mitosis respectively[23, 24].

The earliest event in the ATM –mediated DNA damage response involves ATM and MRN, a complex containing (Mre11, Rad50, and Nbs1). ATM and MRN are recruited to the DNA double stranded breaks (DSBs). Dissociation of ATM homodimers is then induced, and the ATM monomers are recruited to the DNA DSB sites by MRN complex containing (Mre11, Rad50, and Nbs1). ATM phosphorylates histone H2AX which are covering the DSB site. Phosphorylation of histone H2AX is also a part of the early events taking place in DNA damage response, occurring 5-30 minutes after DSB induction. The phosphorylated form is called γ -H2AX, and the phosphorylation of H2AX is spread over an extensive region around the lesion, causing foci formation. Mediator of DNA damage Checkpoint 1 (MDC1), p53 binding protein (53BP1) and BRCA1 are recruited to the phosphorylated H2AX sites[24].

While ATM plays an important role in recognizing DSBs produced by radiation, the ATR mediated DNA damage response pathway is important for Single Stranded Breaks (SSBs) or stalled or broken replications forks. In other words; ATR is crucial for detecting DNA

damage that occurs during normal DNA replication. ATR phosphorylates H2AX in response to these DNA damages, but it also plays a role in the DSB repair after ATM is activated. Short sequences of single-stranded breaks (SSBs) are coated with Replication Protein A (RPA), which recruits ATR and ATRIP. Loading of the sensor Rad17 and 9-1-1 (Rad9, Rad1 and Hus1) leads to full activation of ATR/ATRIP complex, and successful checkpoint function[24] The ATM/ATR-mediated pathways and the consequences are shown briefly in **figure 2.6**. Both ATM and ATR can be involved in the same response.

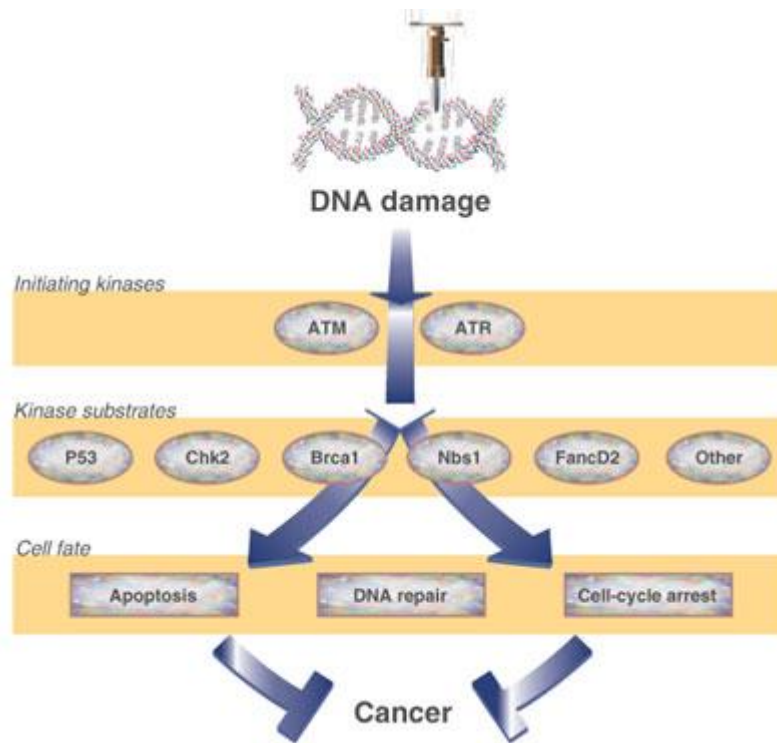


Figure 2.6: DNA damage response. The IR induced-DNA damage pathway and its ultimate consequences for a DNA damaged cell are illustrated in this figure[26].

2.2.2 Cell cycle checkpoints

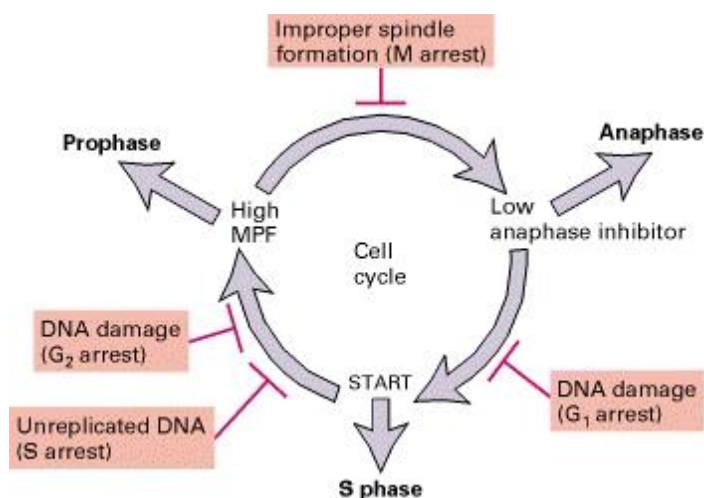


Figure 2.7: Cell cycle checkpoints. The different actions of the checkpoints in the eukaryotic cell cycle are shown above. The DNA-damage checkpoints are G₁, S and the G₂[16] .

Normal eukaryotic cells possess cell cycle checkpoints to ensure that the chromosomes are intact, and to verify that all the phases in the cell cycle are properly completed before continuing to the next phase. The main checkpoint actions are shown in **figure 2.7**.

For DNA –damage control there is three important checkpoints located at the G₁/S transition, S-phase post-replication and at the G₂/M transitions

-G₁/S Checkpoint

At the transition from G₁ phase to S phase the CDK4/6-Cyclin D and CDK2-Cyclin E cooperate in phosphorylating the Rb-repressor complex, which dissociates the Rb transcription factor from the complex. Dissociation of the Rb transcription factor permits transcription of the S-phase genes, resulting in DNA replication and induction of S-phase.

If the cells have DNA damage at the time of G₁/S transition, the checkpoint control system is arresting the cells, prohibiting them from carrying out DNA replication. This checkpoint is activated slowly, and it is shown that it takes about 6 hours to be fully activated. During this period of time, the S-phase entry is not abolished but only slowed[27].

The G₁/S checkpoint responds to growth factor receptor activity and to DNA –damage. In particular, the cell cycle tumor suppressor protein p53 is a very central effector of this

ATM/ATR -DNA damage induced –pathway[28]. At the incidence of DNA-damage the transcription factor p53 is released from the p53-MDM2 complex and activated by ATM/ATR. Activated p53 initiates transcription of several genes, including the p21 Cip1, which works to bind and inhibit CDK2. Since CDK2 is necessary for S-phase entry, the cells remain arrested in G1 phase allowing initiation of damage repair[29]. When the DNA damage is repaired, the cell is allowed to re-enter the cell cycle again[28, 30] .

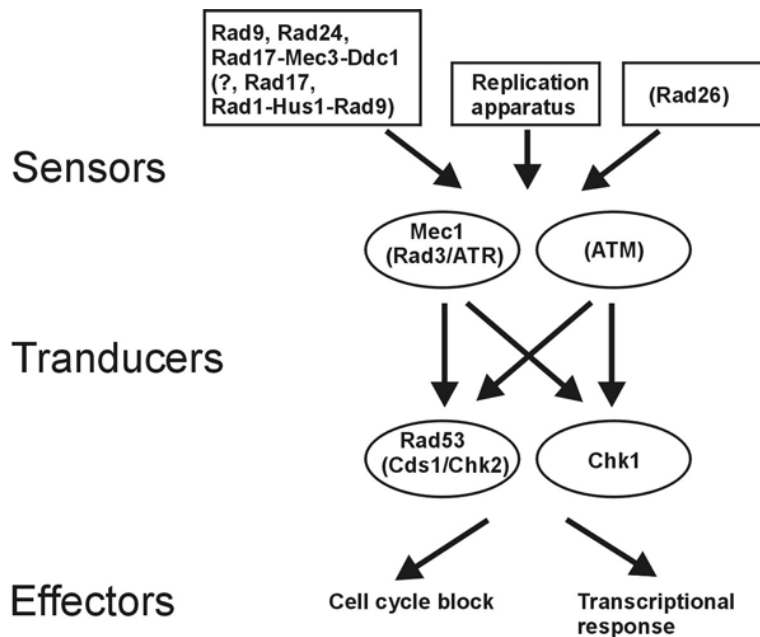


Figure 2.8: S-phase checkpoint. A model of the S-phase checkpoint is shown above. There are two branches of the S-phase checkpoint pathway; both are activated by ATM/ATR.[25]

-S- Phase checkpoint

The S-phase checkpoint is rather inducing a slowing down than a checkpoint arrest. The pathway is initiated by DNA damage and induced activation of ATM/ATR, which works to inhibit Cell Division Cycle 25A (CDC25A) This leads to persistent inhibitory phosphorylation on CDK2 and cell cycle delay.[30] There is also a CDC25A independent pathway which initiates in the presence of DNA damage. It starts with the phosphorylation of NBS1 the product of BRCA1) along with other downstream substrates by ATM[25],

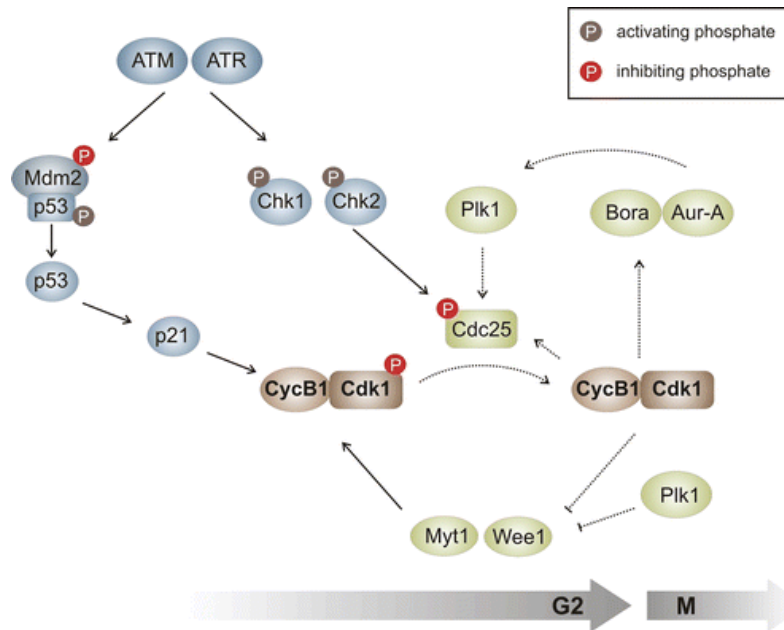


Figure 2.9: G2 checkpoint pathway. The molecular pathways of initiation and inhibition of the G2 checkpoint are shown above[27].

-The G2 checkpoint

The G2 checkpoint ensures that the cell is ready for nuclear division by mitosis. The G2 checkpoint is controlled by the activity of CDK1. By maintenance of the inhibitory phosphorylations on the Thr14 and Tyr15 residues, the CDK1 will be in an inactive state, and the cell will be kept from undergoing mitosis. DNA damage will activate ATM/ATR, which again activates CHK1/CHK2 that in turn will target the phosphatase CDC25 for degradation or nuclear export. The CDC25 phosphatases work to remove inhibitory phosphorylations on CDK1/cyclinB complex added by WEE1/Myt1. The absence of CDC25 leads to increasing levels of inactive CDK1/cyclinB and checkpoint arrest [25, 31].

There is also a p53 dependent pathway activated by ATR/ATM, which initiates the transcription of the p21Cip1 protein, binding CDK1, also resulting in G2 arrest[25, 31].

In addition there are other effectors which work on the CHK1 /2 pathways. The kinases WEE1 and Myt1 work in a feedback loop to add inhibitory phosphorylation on CDK1. Both kinases induce the checkpoint arrest. Unphosphorylated CDK1-cyclinB complex, on the other hand, inhibits both WEE1 and Myt 1. Active CDK1-cyclinB complex also activates the Aurora A, Bora and Plk1 feedback-loop, which activates Cdc25c in removing the inhibitory

phosphorylation on the MPF complex. This results in even more active CDK1-CyclinB, and progress into mitosis[32] . Plk1 is involved in both feedback loops. The mechanisms involved in the G2 checkpoint pathways are shown in **figure 2.9**.

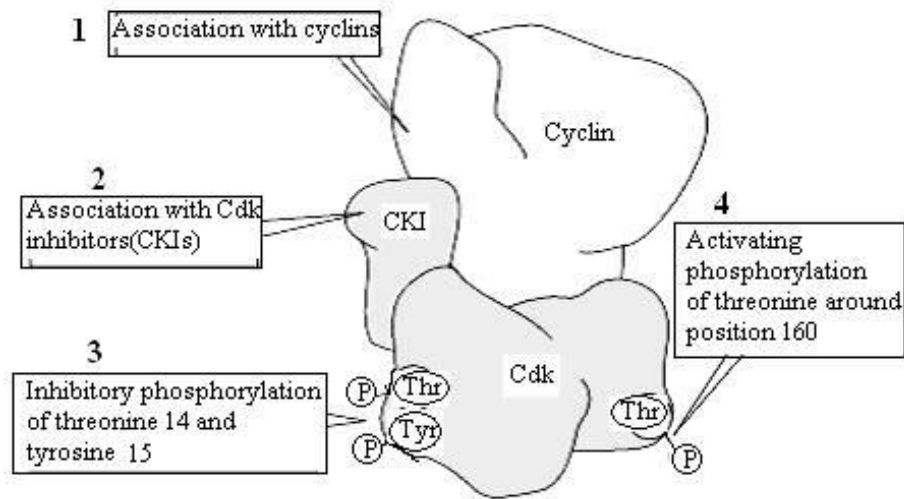


Figure 2.10: The Cyclin Dependent Kinase: The figure illustrates the regulatory sites on CDKs in the cell cycle [33]

The cell cycle is driven by CDK-cyclin activity, and cell cycle control can therefore be performed by tight regulation of cyclin levels and by inhibitory- or activating phosphorylation of CDK, and the CDK-cyclin complexes. The regulatory sites of the CDK are shown in **figure 2.10**.

However, a new concept was introduced in 2002; *Early- and Late G2 checkpoints* induced by ionizing radiation[34]. The early G2 checkpoint is ATM-CHK2-Cdc25a/c dependent, and involves cells in G2 phase at the time of radiation. The checkpoint is rapidly activated after low IR doses, as low as 1Gy is observed, and arrests the cells in the end of G2. The term early checkpoint denotes the drop in mitotic cells at an early time point after radiation[34, 35] **Figure 2.11** shows the cell cycle progression of cells in different phases after IR. “3”, as marked in the **figure 2.11**, is representing the ATM dependent G2 checkpoint. This checkpoint is arresting the cells which were in G2 phase at the time of irradiation, and is denoted the “*early G2/M checkpoint*”. There is also an ATM independent G2 accumulation of cells that were in G1 or S-phase at the time of irradiation, which is called “*The Late G2/M checkpoint*” [34].

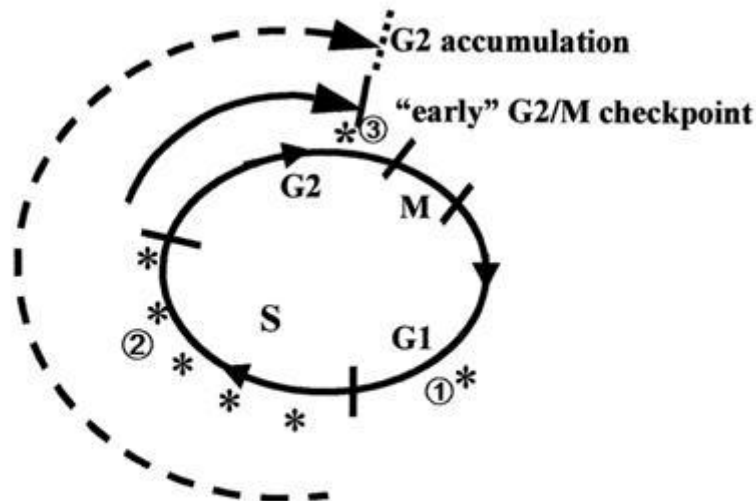


Figure 2.11[34]: Early and late checkpoint. An illustration of the cell cycle progression after IR; Checkpoints are marked with an asterisk.

The late checkpoint applies to cells in G1 or S-phase at the time of radiation. The applicable cells may be affected by G1- and S-phase checkpoints, but they are subsequently delayed in G2 phase, hours after IR, a delay that can last for hours. The late G2 checkpoint is also strongly dose-dependent. Another aspect about the Late G2 checkpoint is the difference from all other checkpoints in being independent of ATM. The checkpoint signaling pathway goes as following; ATR-CHK1-Cdc24a/c, and represents a different type of DNA damage than the one which activates the ATM dependent pathway[35].

2.3 G2-checkpoint and cancer relevance

2.3.1 Loss of Checkpoint, Genomic instability and Cancer development

Cancer development is a consequence of several accumulated genetic mutations. Tumor progression from a single mutation in a single progenitor cell to a tumor is driven by genetic instability[35].

Genetic instability is mutational alterations within the genome which causes a temporary or permanent effect, often in oncogenes or in tumor suppressor genes, and lead to a high risk of developing and accumulation of more mutations. By proliferation, more alterations and mutations are generated in the daughter cells. The mutations that are passed

forward are often giving these cells a growth advantage. For example phenotypes in which a mutated cell can escape death signals or can grow crowdedly at low O₂ conditions (hypoxia). By clonal selection these cells again give rise to new daughter cells with a growth advantage [36]. This is the outlines of the vicious cycle of tumor formation, often consisting of a very homogenous group of cells selected by genetic advantages.

In many types of tumor cells, one or more checkpoints are ineffective or non-functioning due to genetic alterations. Alterations in tumor-suppressor genes coding for p53 and/or BRCA1 are frequently mutated in many cancers[35]. The affected checkpoints in cancers are often G1/S, S and early G2 phase checkpoints, which is described as the provision of extra time for DNA repair. These checkpoints are found to be more important for the quality of the repair rather than the amount of DNA repair occurring. Inhibition of ATR, CHK1, and the late G2 checkpoint is shown to cause radio sensitization in the cells. This makes the late G2 checkpoint a target in anti-cancer therapy, causing increased cell death by cells that prematurely enter mitosis.

2.3.2 Limitation of checkpoints can contribute to genetic instability.

The cell cycle checkpoints are protecting the fidelity of the genome, but they have some limitations. First, the G1/S checkpoint is not able to detect a fraction of cells with DSBs due to slow activation. It is the p53 dependent pathway that delays to initiate. There could be several reasons for this. It has been suggested that the time it takes for the CDK inhibitor p21 to complete post-translational modifications and transcriptional activation is partly the reason for this delay (2-3 hours). The full explanation for the delay is not completely clear, but the effects are causing cells with DSBs to enter S-phase within the 6 hours it takes to fully activate the checkpoint. Consequently, these cells are shown to have a higher level of unrepaired DSBs and chromosome breaks in G2 phase [27].

The G2/M checkpoint is also limited when it comes to detecting DSBs in cells. In contrast to the G1/S phase checkpoint, it responds quickly, but it has a threshold value of 10 to 20 DSBs to initiate cell cycle arrest. Cells with a low number of DSBs will therefore not activate the cell cycle checkpoint, and will be able to progress into mitosis which can lead to loss of genes[27]. A reason for these limitations may be efficiency of proliferation and survival considered against the fidelity of the genome, and the possible risk of mutations and cancer in a multi-cellular organism. In other words, if the checkpoints were too tight,

the rate of cellular proliferation could be too low due to slowing and arresting of minor DNA damaged cells, and that could be a threat itself to the survival of the living organism[27].

2.3.3 Principles of cancer treatment

Ionizing radiation is a common approach for anti cancer treatment, alone or in combination with chemotherapy and/or surgery. IR is generating ions when it is passing through material leading to damaging effects in the cells directly by damaging biomolecules, or indirectly by reacting with water, generating free radicals or reactive oxygen species. In its ultimate form, IR induced damage is leading to cell death and or apoptosis[37, 38] .

Another approach is to target the cell cycle DNA damage checkpoints in combination with IR/chemotherapy or other DNA damaging agents. By first induce DNA damage to the cell, and then target checkpoint inducers, will lead to preventing checkpoint initiation and DNA repair.

2.3.4 G2 checkpoint as a therapeutic target

Many cancer cell lines are G1/S checkpoint deficient due to lack of p53. Therefore, these cells rely only on S-phase checkpoint and the G2/M checkpoint for DNA damage repair[38]. S-phase checkpoint is rather slowing down the damaged cells than arresting. Thus, an abrogation of S-phase checkpoint would result in no slowing down in S-phase of cancerous cells ,only to arrest at the G2 phase checkpoint. Abrogation of the G2 checkpoint of DNA damaged cancer cells will induce a premature mitotic entry leading to apoptosis and mitotic catastrophe, a special form for cell death with multiple micronuclei, nuclear fragmentation and dysentery chromosomes[35]. Normal cells with a functioning G1/S checkpoint will not be affected by G2/M checkpoint abrogation in the same way as many cancer cells which are only relying on one checkpoint. This approach is thought to spare normal tissue to a greater extent.

The mitotic catastrophe is a term describing cell-death during mitosis and is connected to abnormal MPF activation. The pathway is a different one than the one executed for apoptosis, and it is p53 independent. The mitotic catastrophe is preventing the cells from developing genetic instability by forming aneuploid daughter cells. However, cell death during metaphase/anaphase transition is involving some of the hallmarks of apoptosis; by

the activation of caspase-2 and/or – permeabilization of the mitochondrial membrane releasing more death inducing effector[39]. In this way, the mitotic catastrophe is found to be related to apoptosis, but in contrast to apoptosis, the mitotic catastrophe is caspase-independent in an early stage of the pathway[35, 39].

2.3.5 WEE1-inhibitor

WEE1 is found to be over expressed in several types of cancer such as some types of breast cancer, glioblastoma (GMB), colon- and lung carcinoma, seminoma, and osteosarcoma(OS)[1, 40]. *WEE1* is inducing G2 phase arrest by adding inhibitory phosphorylation to the CDK1-cyclinB (MPF) complex, and inactivating it. *Consequently, abrogation of the G2 checkpoint is forcing DNA damaged cells to continue to cycle, and which ultimately leads to apoptosis and mitotic catastrophe.* If *WEE1* is inhibited, it is shown that a greater fraction of cells are prevented from arresting, and will therefore enter mitosis prematurely. *WEE1* inhibitors (MK1775) or silencers (si*WEE1*) are both currently in clinical trials stage 1, in combination with anti-cancer agents (cisplatin, carboplatin, gemcitabine, 5-fluorouracil) abolishing the phosphorylation of the tyrosine 15 residue on CDK1. All experiments are showing abrogation of the G2 checkpoint and premature mitotic entry, followed by a mitotic catastrophe, in the case of *WEE1* the depleted cells[41].

Preclinical studies with cancer cell lines and animal models have shown that *WEE1*-depletion by a small molecule *WEE1* inhibitor or by si*WEE1*, lead to increased tumor-cell death, reduced tumor burden and increased survival .The *WEE1* depletion was performed in combination with DNA damaging agents such as IR and/or cytostatics. p53 deficient cells lines were in particular sensitized to DNA damage treated with such combination therapy. Moreover, one of the *WEE1*inhibitors is currently in clinical trials[42].

2.3.6 CHK1- inhibition or silencing

CHK1 is also a molecule highly involved in a series of DNA damage checkpoints, and it is activated by agents causing double stranded breaks and those causing replication stress. CHK1 is therefore involved in intra S-phase- and G2/M -DNA damage checkpoints.

CHK1 works to phosphorylate CDC25 (A, B or C) dependent on which checkpoint.

Phosphorylation of CDC25A leads to ubiquitination and degradation, prohibiting activation

of cyclin-CDK complex. On the other hand, phosphorylation of CDC25B or C are creating a binding site for the 14-3-3 phospho serine binding proteins which are isolating the CDC25 protein in the cytoplasm, and prevent interaction with Cyclin-CDK complex. CDC25 interaction with cyclin-CDK complex will cause removal of inhibitory phosphorylations of cyclin-CDK complex, and activation of the complex driving the cell cycle forward[43].

CHK1 has been a target in G2/M checkpoint abrogation, due its crucial role in both S-phase and G2/M checkpoint. In addition to this, CHK1 is also necessary for the mitotic spindle checkpoint function. Inhibitors of CHK1 are shown to enhance the effect of DNA damaging agents that cause S or G2 arrest, in addition to amplify anti-mitotic activity. Furthermore, CHK1 inhibition has an effect on tumor cells with cell-cycle mediated drug resistance, it may eliminate this type of resistance. CHK1 inhibitors are in use in early clinical studies[43].

2.4 mRNA silencing

2.4.1 SiRNAs

Short double stranded RNA molecules are involved in RNA interference (RNAi) and can be targeted to interfere with the expression of a specific gene. Thus genetic diseases, viral diseases and cancer are diagnosis which is applicable for siRNA-therapy research.

Small interfering RNA/silencing RNA (siRNA) is formed from segmenting a long double stranded RNA in the cytoplasm. The segments are processed by an RNase III-like enzyme called DICER producing siRNA, which is 20-25 nucleotides in length and with two nucleotide overhangs on the 3' end[44]. The processed siRNA then associates with several proteins to form a multi-subunit protein complex called RNA-induced silencing complex (RISC). The binding of siRNA to the complex is ATP dependent[44]. The RISC contains active endonucleases (agronaute) proteins involved in cleavage of phosphodiester bonds in RNA[45]. The antisense strand remains bound to the RISC complex, while the complementary strand is removed by the agronaute protein, Ago-2 [46]. RISC is then guided to the complementary target mRNA sequence. The mRNA strand binds to the antisense strand associated with the RISC complex, following cleavage by Ago-2. In other terms, leading to sequence directed

removal of the particular mRNA transcript, and down regulation of the target gene expression[44]. However, one drawback of using siRNA silencing is the risk of off-target effects. Off-target effects can occur in the sense that siRNAs can pair with, and alter unintended genes. Consequently, co-depletion of unintended targets can lead to altered phenotypes. Most of the off-target effects have to do with homology in the 3' untranslated Region (3'UTR) following the coding region of the mRNA to the seed region, (nucleotides 2-8) in the siRNA[47]. A study found that there is an error-rate of off-target effects at about 10 %. The same study could also demonstrate that the nucleotide length with highest specificity and lowest off-target effect were found to be 21 nucleotides long, the same length mostly found *in vivo*[48].

Another obstacle is unintentional cleavage of siRNA at vulnerable sites. This can be overcome by special modifications at these sites, which do not interfere with the action of the siRNA[49]. Another challenge is delivery of siRNAs *in vivo* to the specific organ, and into the cytoplasm of the cell. RNA cannot penetrate the cell membranes, due to negative charge and size, leading to unsuccessful systematic delivery. RNases in the serum would rapidly degrade the siRNAs, even the modified siRNAs. Thus, other methods are developed for delivery of siRNAs; viral delivery, using nanoparticles or liposomes, bacterial delivery or chemical modifications[50].

Liposomal transfection includes siRNA containing liposomes which delivers the siRNAs to the cell cytoplasm by the endosomal pathway fusing with the cell membrane.

Oligofectamine and Lipofectamine are examples of such liposomal transfection reagents.

The reason for why siRNAs in treatment of diseases are currently being investigated is its role in offering a reversible, transient and drug-like approach for treatment of many diseases. Also, the use of RNA-antisense strategy is a more sensitive method than using DNA oligonucleotides and ribozymes. This means that the RNA-effector molecules work at much lower concentrations[46] Treatment with siRNAs is currently in early clinical trials. But there are currently some obstacles to be solved, like off-target effects[47]. It remains to design modified siRNAs in order to minimize off-target effect, and maximizing the specificity and delivery[51].

2.4.2 EsiRNAs

Endoribonuclease-prepared siRNAs (esiRNAs) are, as the name is revealing, a mixture of siRNAs cleaved by an endoribonuclease. The esiRNAs are pools of siRNAs 18-25- base pairs in length, produced by *E.coli* RNase III, or the enzyme DICER. This cleavage is generating overlapping siRNA fragments[52] **Figure 2.12** shows the steps of synthesis in details. The advantage of esiRNAs over normal siRNAs is reduction of off-target effects caused by homologies in non-target mRNA and siRNAs. The complex mixture of many siRNA fragments is sharing the same target mRNA, but differing in their off-target signatures. Since the off-target signature is sequence determined, a high degree of silencing of the target is obtained at the same time as the off target effects are diluted[53].

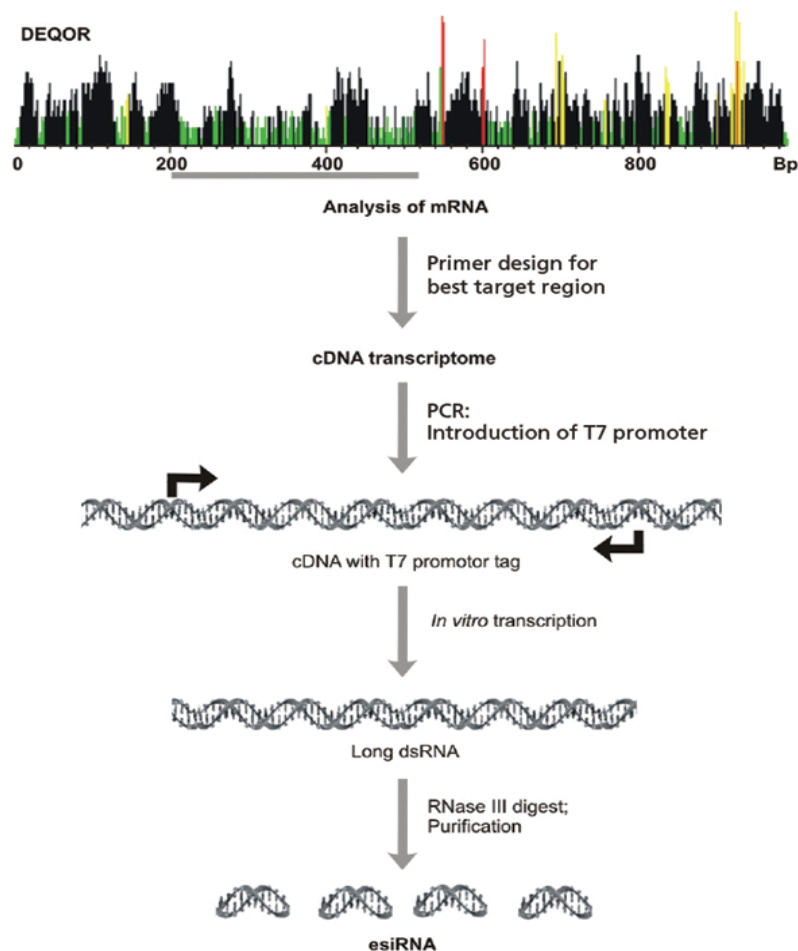


Figure 2.12: esiRNA synthesis. The stages of esiRNA synthesis are shown above.[52]

3. Materials, chemicals and instruments

The chemicals, reagents and instruments that were used in this project are shown in **tables 3.1-3-6**. Reagents and buffers are sorted by experiment and are shown in **table 3.1** and **3.4**. Primary- and secondary antibodies are listed in **tables 3.2** and **3.3** respectively. EsiRNAs, siRNAs and the WEE1 inhibitor is shown in **table 3.5**. **Table 3.6** is listing the instruments and software that has been used throughout the experiments.

Table 3.1: This table is listing the reagents that are applied in this project by type of experiment.

Reagents /specification	Catalogue number	Supplier
Cell cultivation/Cell cycle experiments		
U2OS-VP16 Cells U2OS cells expressing normal, wild-type p53		
U2OSp53dd cells p53 deficient cells, expression of dominant-negative mutant p53		
1xPBS pH7.2 (GIBCO)	20012	Invitrogen
DMEM+GlutaMAX (GIBCO)	31966	Invitrogen
FBS (GIBCO)	10270-106	Invitrogen
Penicillin Streptomycin	15140-122	Invitrogen
Trypsin-EDTA (0.25%Trypsin)	25200-056	Invitrogen
G-418	A1720-5G	SIGMA
Tetracycline	T7660-5G	SIGMA
Puromycine	P8833-10MG	SIGMA
Effectene Transfection Reagent KIT	301425	QUIAGEN
Oligofectamine transfection reagent	12252-011	Invitrogen
OPTI-MEM I (GIBCO)	151985-026	Invitrogen
Nocodazole (0.04mg/mL) dissolved in DMSO	M1404	SIGMA
Hoechst 33258	H3569	Invitrogen
Vectashield mounting medium (Containing DAPI nuclear stain)	H-1200	Vector
Protein Quantification		
Micro BCA Protein Assay Kit	23235	Thermo Scientific
Western Blotting		
Precise Protein Gels 4-20% (15 wells)Pierce Protein Research Products	25244	Thermo Scientific
Ponceau S solution(0.1% Ponceau S(w/v) in 5%(v/v) acetic acid)	P7170	SIGMA
Amersham Hyperfilm ECL	28906837	GE Healthcare
SuperSignal West Pico Chemiluminescent Substrate	34080	Thermo Scientific
SuperSignal West Dura Extended Duration Substrate	34075	Thermo Scientific

Table 3.2: This table is listing the antibodies and their specifications, used in this project.

Primary antibodies	Clone number/gene ID	Catalogue number	Supplier
Mouse anti-MCM7	DCS-141		Santa Cruz
Rabbit anti-Cyclin A (H-432)	/890	sc-751	Santa Cruz
Mouse anti-Cyclin B1 (GNS1)	/891	sc-245	Santa Cruz
Rabbit anti-Cdk1-P-Tyr 15 (Cdc2-p-Tyr15)(10A11)	/983	4539	Cell Signaling
Rabbit anti-SSH3 311	/54961	A301-311A	Bethyl
Mouse anti-Chk1	DCS 310.1	ab49383	Abcam
Rabbit anti-γ-tubulin	6-11B-1	T5192	SIGMA
Mouse anti-γH2AX ser139	JBW301	05636	Millipore
Rabbit anti-H3 ser10p	/NP_003484.1	06570	Millipore
Rabbit anti-53BP1	/27223	ab36823	Abcam
Mouse anti-RPA	9H8	MS-691-P1ABX	Thermo Scientific

Table 3.3: This table is listing the antibodies and their specifications, used in this project

Secondary antibodies	Catalogue number	Supplier
Peroxidase labeled anti-mouse, IgG (H+L)	PI-2000	Vector
Peroxidase labeled anti-rabbit, IgG (H+L)	PI-1000	Vector
Anti-mouse Alexa 488, IgG (H+L)	A21202	Invitrogen
Anti-rabbit Alexa 568, IgG (H+L)	A10042	Invitrogen
Secondary antibodies	Catalogue number	Supplier
Peroxidase labeled anti-mouse, IgG (H+L)	PI-2000	Vector
Peroxidase labeled anti-rabbit, IgG (H+L)	PI-1000	Vector
Anti-mouse Alexa 488, IgG (H+L)	A21202	Invitrogen
Anti-rabbit Alexa 568, IgG (H+L)	A10042	Invitrogen

Table 3.4: This table is listing the reagents and the buffers in this project

Reagent/Buffer sorted by experiment	Contents :
Antibody staining for flow cytometry	
Detergent buffer:	
	0.1% Nonidet P40 (Igepal CA-630)
	6.5mM Na ₂ PO ₄
	1.5 mM KH ₂ PO ₄
	2.7nM KCl
	137 mM NaCl
	0.5mM EDTA pH 7.5
	4% w/v nonfat milk
Western Blotting	
4x Leammli Sample Buffer (LSB):	
	1mL 1M Tris pH 6.8
	2mL 1M DTT
	0.4g SDS
	2mL Glycerol
	5mL Bromphenol blue
Boiling lysis buffer:	
	2% SDS
	10mM Tris-HCl,pH 7.4
	1mM Na ₃ VO ₄ (-20C)
10x Running Buffer:	
	30mM SDS
	1M HEPES
	1M Tris ,pH 8.0

Continuation on Table 3.4: This table is listing the reagents and the buffers in this project

Reagent/Buffer sorted by experiment	Contents :
1x Running Buffer :	
	10x Running Buffer diluted 1:10 in distilled water
10x Transfer stock buffer:	
	1.92M Glycin (144g)
	250mM Tris Base(30.3g)
1x Transfer buffer (1L):	
	700mL distilled water
	200mL Methanol
	100mL 10x stock buffer
PBST (washing solution) :	
	5mL Tween 10%
	495 mL 1xPBS
Blocking solution :	
	2.5 g non-fat milk powder
	50 mL PBST

Table 3.5: This table is showing the specifications of the siRNAs, esiRNAs and the WEE1 inhibitor used in this project.

siRNAs/esiRNAs/ Inhibitors	Specification	Catalogue number	Supplier
siRNAs:			
siCHK1	Sequence: 5'GGGAUUAUAAAACCAGAAAA[dT][dT];		SIGMA
siSSH3	Dharmacon Human SSH3	D-008937- 04	Thermo Scientific
esiRNAs:			
esiCHK1	MISSION esiRNA	EHU05614 1-50 UG	SIGMA
esiSSH3	MISSION esiRNA	EHU08512 1-50UG	SIGMA
esiDUSP16	MISSION esiRNA	EHU15736 1-20UG	SIGMA
esiPTP7	MISSION esiRNA	EHU08650 1-20UG	SIGMA
WEE1i inhibitor:			
MK1775		Axon 1494-5MG	Axon

Table 3.6: This table is showing the specifications of the equipment used in this project

Description	Name	Supplier	Other
Fluorescence microscope	Imager Z1	Zeiss	Vistec Inc VIP3200-z-008
Structured illumination for wide field fluorescence microscopy	Apo Tome	Zeiss	
Microscope camera	AxioCam MRm	Zeiss	
Fluorescence microscope software	AxioVision 4.0	Zeiss	
X-ray machine	Faxitron X-ray CP160	Imitios medical AB	SID1040
Spectrophotometer For MicroBCA	PowerWave XS2	BioTek	MQX200R2
Software for BCA analysis	Gen5	BioTek	
Flow Cytometer	BD LSR II	BD Biosciences	
Software for Flow Cytometry analysis	BD FACS Diva 6.0	BD Biosciences	

4. Methods

4.1 Cell cultivation

U2OS cells expressing normal, wild-type p53, and U2OSp53dd, p53 deficient cells (due to expression of dominant-negative mutant p53) were grown as described below. The cell - cultures were grown in flasks in liquid medium. The cultures were investigated by microscopy frequently to look for confluence, and splitted when needed. U2OS and U2OSp53dd cell lines are adherent cells, which needs to be detached from the base of the growing flask before splitting. For experiments, the desired number of cells was plated on either 35mm- or 60mm diameter dishes.

- DMEM +10% FCS (Penicillin-Streptavidin) growth medium, PBS, trypsin (all sterile) warmed up in water bath to 37C.
- The liquid medium in the growing flask were removed.
- The flask was then washed with PBS.
- Detachment of cells were performed with 2 ml trypsin ,and incubated 2min at 37C
- The cells were re-suspended in the growth medium and diluted as preferable. In total 10 mL cell culture and medium in a T75 flask
- U2OSp53dd cells: Added antibiotics : Tetracycline (2 µl/ml medium),Puromycine (1 µl/ml), G418 (1 µl/ml)

4.2 Effectene esiRNA transfection

Effectene is originally meant for DNA-transfection, however it is recommended for use for esiRNA transfection of U2OS cells by The Max Planck Institute for Cell Biology and Genetics' esiRNA homepage[53]. The outlines of the transfection protocol are shown in **figure 4.1** and are taken from the *Effectene Transfection Reagent Handbook*[54]. The esiRNA stocks were all having the same concentration at 200ng/ μ L RNA. Different conditions were tried out to optimize Effectene transfection. The various conditions, **a**, **b**, **c** and **d** of esiRNA and Effectene concentrations tried out in the experiments are shown in **table 4.1**.

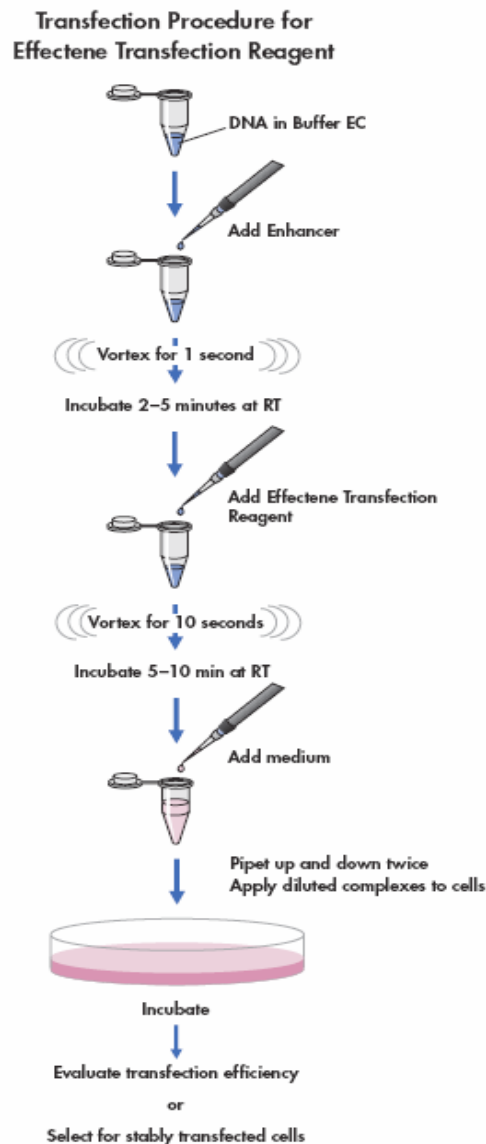


Figure 4.1: The outlines of Effectene transfection are shown in the figure above. [54]

1×10^5 U2OSp53dd cells/35mm dish were plated approximately 24h before transfection. DMEM +10% FCS (P-S) growth medium were used for Effectene transfection. The Effectene Transfection Reagent KIT is containing: Buffer-EC, Enhancer and Effectene Transfection reagent. The protocol shown below is valid for 1x35 mm dish. For 1x60mm dish, the conditions are multiplied by a factor of 2.5, including reagents and the number of cells.

- The old growth-medium was removed in the dish with growing cells, and 1.6 mL fresh medium was added/dish.
- 100 μ L EsiRNA-Buffer EC solution was added to an Eppendorf tube. The volumes of esiRNA are shown in **table 4.1**. To compensate for varying volumes of esiRNA, sufficient volume of Buffer EC was added in order to obtain 100 μ L total volume.
- Then Enhancer was to the tube.
- Vortexed Eppendorf tube for 1 sec.
- Incubated 5 minutes at room temperature.
- Added Effectene Transfection Reagent
- Vortexed for 10 sec.
- Incubated 10 min. at room temperature.
- Added 600 μ L medium to the tube, and pipetted up and down twice.
- Then, 600 μ L of the solution was added drop wise to a 35mm dish with growing cells.

Samples were collected at 48h or 72h post-transfection.

Table 4.1: Showing different conditions for optimization of Effectene transfection

	esiRNA [μ l]	Enhancer [μ l]	Effectene [μ l]
a	10	3,2	10
b	10	3,2	5
c	5	3,2	10

4.3 Oligofectamine siRNA transfection

1×10^5 /35 mm dish U2OSp53dd cells were plated approximately 24hours before.

The protocol is valid for 1x35mm diameter dish. For 1x60mm diameter dish, the conditions including the number of cells plated are multiplied by a factor of 2.5.

Cell culture medium without P-S (DMEM medium +10% FCS) was used for Oligofectamine transfection

- The old growth-medium was removed in the dish with growing cells, and 800 μ L fresh DMEM medium +10% FCS was added/dish.
- 2 μ L Oligofectamine and 13 μ L Optimem were added to an Eppendorf tube, **A**
- 1.25 μ L siRNA (with stock concentration of 20 μ M) and 175 μ L Optimem were added to a second Eppendorf tube, **B**, and incubated 7minutes at 37C.
- **A** was then added to **B**, and incubated for 20 min at room temperature.
- 200 μ L of the mixture(**A+B**) were then added drop wise to each dish
- Samples were collected at 48h or 72h post-transfection.

4.4 WEE1 inhibition

1×10^6 U2OS-or U2OSp53dd-cells /6cm dish were plated approximately 24h before. DMEM +10% FCS (Penicillin-Streptavidin) growth medium were used for cell growth at WEE1 inhibition, and for dilution of MK1775.

- Diluted appropriate concentration of WEE1inhibitor (MK1775) in medium and the different conditions that were applied are shown in **table 4.2**.
- Added drop wise 3mL of the dilution to the dishes with growing cells. Incubate d 15 min at 37C.

Table 4.2: Showing different conditions for WEE1inhibitoion with MK1775

Concentration MK1775 [nM]	MK1775[μ L]/mL medium
mock	0
100	1
300	3
1000	10

4.5 IR

Irradiation of samples were performed 15 minutes after siRNA/esiRNA transfection or WEE1inhibition; the irradiated samples were treated with 6Gy in the *Faxitron X-ray CP160* (160kV) described in **table 3.6**.The dose rate is 1 Gy/min and with 6, 3 mA.

4.6 Early versus Late G2 Checkpoint

Experimental setups for inhibition/transfection late and earlyG2 checkpoint -experiments are shown in **figure 4.2(a)**,while the setup for siRNA/esiRNA transfection are shown in **figure 4.2.(b)**

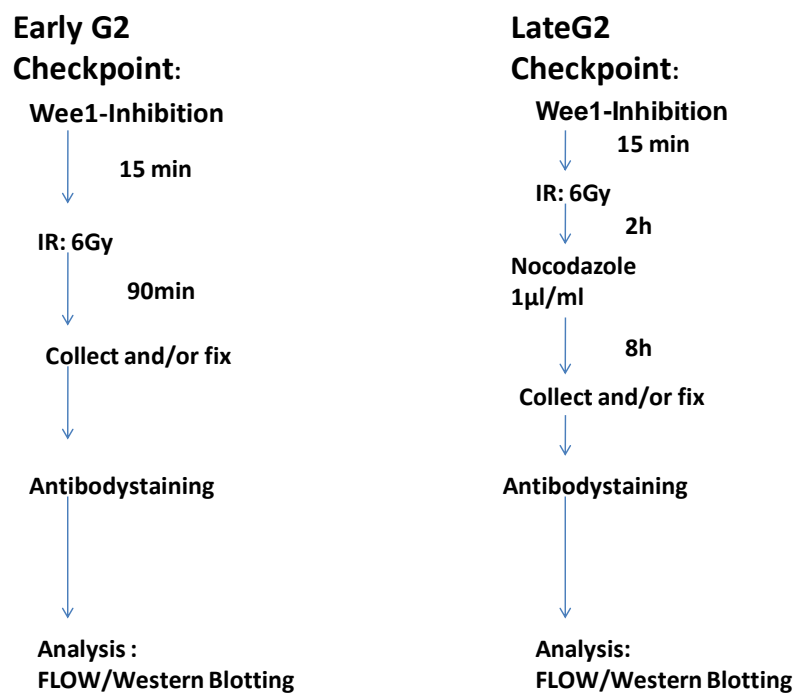


Figure 4.2(a): Early-and late G2 checkpoint experiments. An overview over experimental setup for “early” and “late” G2 checkpoint inhibition and transfection experiments is shown above.

siRNA/esiRNA transfection

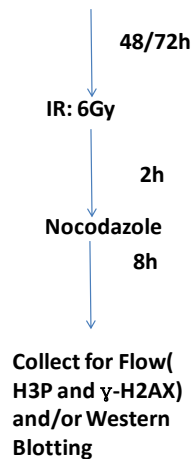


Figure 4.2(b): Si/esiRNA transfections. The setup for siRNA/esiRNA transfection experiments are shown above.

Early checkpoint experiments were harvested 90 min after IR treatment. Late checkpoint experiments were treated with Nocodazole 2 h post-irradiation, and fixed 10 hours after IR. After fixation the samples were stained with antibodies and analyzed by Flow Cytometry or Fluorescence microscope for phenotype, or Western Blotting for genotype. The details in these steps are described in the **sections 4.7 -4.13**, below.

4.7 Harvesting and Fixing

After transfection/inhibition of cells:

- First, the medium in the dishes were collected in order to harvest the mitotic, unattached cells. The medium were transferred to a 15 mL tube per sample.
- Then washed with PBS, and collected the PBS to the respective tube.
- Added 1mL Trypsin, and incubated 2 min in 37C
- Added medium and re-suspended solution in order to archive a single cell solution
- Collected cell solution in the 15mL tubes and spin
- Removed supernatant
- Added ice cold ethanol (-20C, 70%) drop wise while vortexing . 1mLEtOH/tube
- Store at -20C (minimum 1hour, or long term storage)

4.8 a) Immunostaining for Flow Cytometry

- The cells were fixed in 70% EtOH, -20C, prepared as described under section **4.7**.
The fixed cells are in 15 mL tubes
- The 15 mL tubes filled with PBS 1% FBS and spun
- Then the supernatant were removed equally in each tube
- The pellet was resuspended in 50 μ L detergent buffer with 4 w/v % milk. Left for 5 minutes at room temperature
- Added 50 μ L of appropriate primary antibody solution in each tube. The antibodies were diluted in detergent buffer. (Mouse anti γ -H2AX diluted 1:250 and rabbit ser 10p diluted 1:250, which gives a final dilution of 1:500) .Incubated 1hour at room temperature.
- Filled the tubes with PBS 1% FBS, spun.
- Removed supernatant equally in each tube
- Added 100 μ L of secondary antibody diluted in detergent buffer (Alexa anti-rabbit 488 and Alexa anti-mouse 647 diluted 1:500)
- Filled tube with PBS 1% FBS. Spin.
- Removed supernatant and added 500 μ L Hoechst in PBS (2.4 μ L Hoechst /ml PBS stock)
- Stored dark at 4C until analyzing. Minimum 30 minutes and maximum overnight.

- The samples were analyzed with a Flow Cytometer; *BD LSRII* and *FACS Diva software*. The most important principles from analysis of the histograms form the software are shown below, in **section 4.8 b**).

4.8 b) Flow cytometry analysis

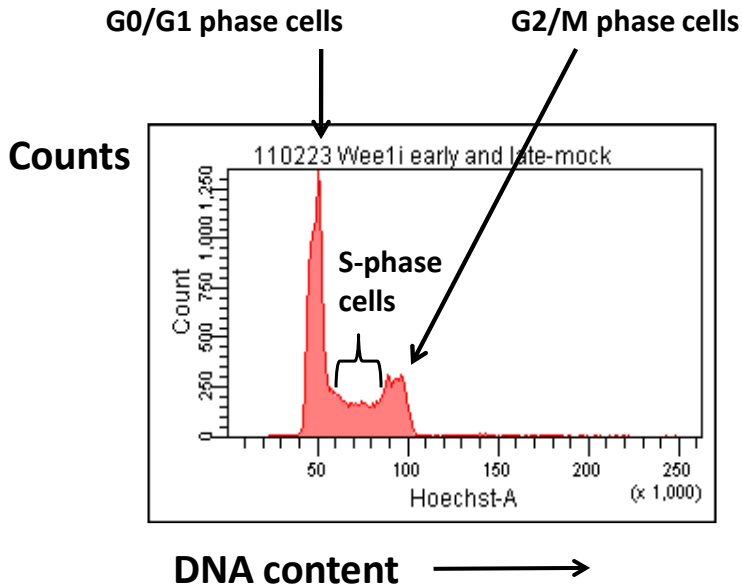


Figure 4.3: Normal cell cycle. The normal cell cycle distribution is shown above as a function of DNA content.

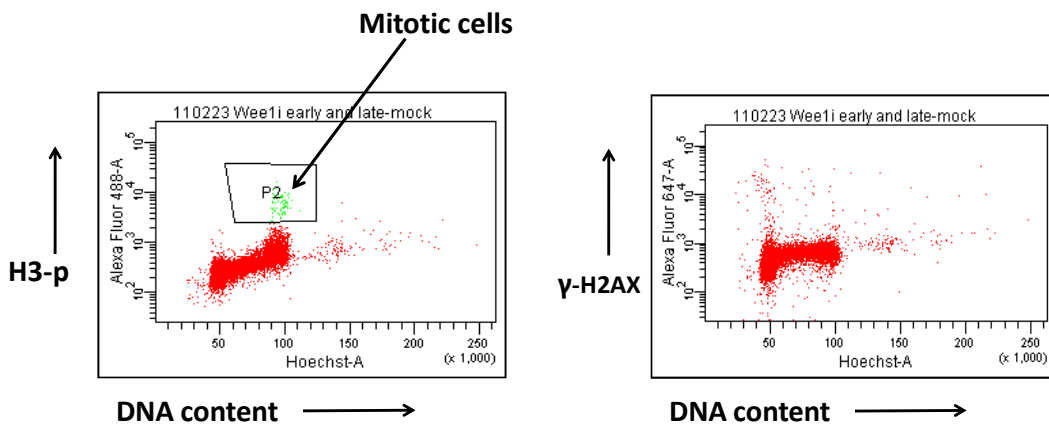


Figure 4.4(a) and (b): (a) H3-p and γ -H2AX .Flow cytometric analysis of G2 abrogation by measuring the fraction of H3-p positive cells. The mitotic cells are gated, showing in the P2 area. (b) Flow cytometric analysis of the distribution of DSBs measured by median γ -H2AX levels. Both figures are showing non-irradiated cells-

The histograms and two-parameter plots of greatest importance obtained by the FACS software by analysis of samples are shown in **figures 4.3, 4.4(a, b)**. In **figure 4.3**, a representative distribution of a normal cell population is shown as a function of DNA content. The first peak denotes G0 and G1 cells together since they contain the same amount of DNA. The area in between the two major peaks represents S-phase cells. S-phase includes a wider specter of DNA contents, depending on how far the cell has come in replication of the DNA. The second peak is counting both G2 and M phase cells, since

their DNA contents are the same. In this thesis, it is of interest to look at the mitotic fraction (MI) of cells, therefore the G2 cells must be separated from M cells. To distinguish between G2 and M phase cells, cells were co-stained with an antibody to phospho-H3, a mitotic marker. **Figure 4.4(a)** is showing the amount of detected Alexa Fluor 488, which is according to the amount of H3-p. The region P2 is gating the H3-p positive cells, giving the MI. **Figure 4.4(b)** is of interest to confirm that the cells have IR induced DSBs, and an activated G2 checkpoint at an early stage. This is confirmed by an elevated median γ -H2AX level compared to the non-irradiated cells.

4.9 Immunostaining of Coverslips for Immunofluorescence microscopy

1×10^6 U2OS and U2OSp53dd cells/ 60mm dish plated approximately 24h before. 05.04.11
 $0,5 \times 10^6$ cells in 35mm dishes plated approximately 24h before.

The proper amount of cells was first plated. Then they were transfected with WEE1i (MK1775) 300nM for 10 hours before they were fixed in Paraformaldehyde and stained for Immunofluorescence. Primary antibodies for γ H2AX and 53BP1 were diluted in DMEM+ 10% FCS+ P-S, growth medium.

- Permeabilization of cells:
- Dishes were left 2 minutes on ice with 70% MeOH (-20C), and washed 3x with PBS
- 100 μ L of the primary antibody solution added to each coverslip,
- Coverslips incubated 1hour at room temperature.
- Then the coverslips were washed 5x with PBS.
- Added 100 μ L secondary antibody solution to each coverslip. Incubated 30 min. room temperature.
- For both antibody sets:
- Secondary antibody solution: anti-mouse Alexa 488 and anti-rabbit Alexa 568. Both diluted 1:1000 in same solution.
- Washed 3-5x with PBS and 1x with distilled water (extra pure). Air dried
- Coverslips were mounted on coverglass using Vectashield and cells facing downwards. Sealed the coverslips with nail polish, and stored dark at 4C.

The samples were analyzed by microscope; *Zeiss, Imager, Z1, Vistec Inc VIP3200-Z-008 B002544* with *Zeiss, Apo Tome* and camera; *Zeiss, Axiocam MRm*. The software: *Axio Vision 4.0*.

4.10 Prior to cell lysates preparation

- First, the medium was removed from the dishes, and discarded.
- The dishes were washed with 2mL cold PBS x2, and removed.
- Afterwards the dishes were taped and transferred them immediately to a freezer (-80C), in order to crack the cytoplasmic - and the nuclear membrane.

4.11 Cell lysate preparation

- Prepared 100µL boiling lysis buffer per 35mm dish.
- Added 100µL boiling buffer to the first dish, and kept the others on ice.
- Then scraped the cells until a viscous solution was obtained.
- The cell suspension was added to an Eppendorf tube, and kept on ice.
- The tubes were then boiled at 95C for 10 minutes. If the content was sticky after boiling treatment, more boiling buffer was added, and the tubes were re-boiled.
- Stored at -20C.

This procedure was followed by analysis by protein quantification and/or Western Blotting.

4.12 Protein Quantification

BSA standard for microBCA+ Micro BSA kit are used for protein quantification, containing reagent A, B and C.

Cell lysate obtained and prepared as described under **section 4.10** and **4.11**.

The analysis were performed in 96-well plates-

- 200µl /well of 160µg/mL BSA (diluted albumin) standard were added to wells A1,A2 and A3
- The wells A (1, 2, 3) –F (1, 2, 3) were then diluted respectively 1:2 in ddH₂O as shown in table 4.3. Wells H(1,2,3) are blanks
- 1:100 and 1:200 dilutions of each lysate sample were prepared.
- Then two parallels of each dilution were added to four separate wells. In total 100µL in each well.
- 5mL of reagent A + 4.8 mL of reagent B + 0.2mL of reagent C were mixed.
- Then 100µL of the solution from step 5 was added to each well to initiate a colored reaction.
- The samples were then incubated at 37C for 2 hours
- Analysis was performed by BioTek Power Wave XS2 Spectrophotometer at 562 nm. The software for Micro BCA analysis Gen5 and the output were used to generate a standard curve, which by regression analysis can be used to determine the concentration of the particular sample.

Table 4.3 Concentrations of BSA standard [µg/mL] for protein quantification in a 96-well plate

Well #	1	2	3
A	160	160	160
B	80	80	80
C	40	40	40
D	20	20	20
E	10	10	10
F	5	5	5
G	2,5	2,5	2,5
H	water	water	water

4.13 Gel electrophoresis, Western Blotting and immunodetection

$0,5 \times 10^6$ cells/ 35mm dish were plated for these experiments.

Amersham ECL Western Blotting Detection System or Amersham ECL Plus Western Detection System Containing solution 1 and 2 were used to prepare for developing.

- **Sample preparation:** Cell lysate was obtained and prepared as described under **section 4.10** and **4.11** and then thawed.
- 5 μ L 4xLSB buffer was added to 10 μ L of each sample, and then they were boiled at 95C for 5 minutes and spun.
- **Gel electrophoresis.** The electrophoresis container, the ice, the 15-well 4-20% Precise Protein Gel and the electrodes were assembled and connected.
- 1x running buffer was prepared from 10x running buffer, and added to the electrophoresis container.
- 5 μ L full-range Rainbow marker was added to the first and the last well. 15 μ L of the sample were added to the other wells.
- The gel electrophoresis was run at 100V for 1 h 10 min, at room temperature.
- **Transfer of proteins and staining (Western Blot).** 1x Transfer buffer were prepared and added to the transfer box with a magnetic stirrer.
- The blotting cassette were assembled, and placed together with an ice cube into the transfer box.
- The electrodes were placed correctly, and an electrical force was connected. Run at 100V for 1h 10 min, at 4 C.
- The protein bands in the membrane were the visualized staining with Ponceau S solution for 5 min.
- The membrane was the left for blocking in Blocking Solution at a shaker for minimum 1h.
- Primary antibodies with appropriate dilutions were added to the membrane. Diluted in PBST-milk. Enough antibody solution to keep the membrane from drying out. Incubated in a humid chamber over night at 4C.
- The primary antibodies were washed off 3x10 min in Washing Buffer on shaker.

- Appropriate secondary antibodies (anti-mouse or anti-rabbit, both IgG) were added in a dilution 1:10 000. Diluted in PBST-milk. Enough antibody solution to keep the membrane from drying out. Incubated 30 min. at room temperature.
- The secondary antibodies were washed off 3x10 min in Washing Buffer on shaker.
- **Detection.** Amersham ECL Western Blotting Detection System or Amersham ECL Plus Western Detection System were applied to the membranes as following
- Solution 1 and 2 were first mixed 1:1. (typically 3mL of each)
- Enough mixture were added to cover the surface of the membranes, and were incubated for 5 minutes
- Membranes were then dried quickly with paper towels and wrapped into plastic foil
- The wrapped membranes were inserted into a cassette
-
- In the dark room, Amersham Hyperfilm ECL developing film were added to the Kodak cassette .The exposure time were adjusted to each membrane in order to get the best result.
- **Developing.** Developed films in a *developing machine* in the dark room.

5. Results

“No amount of experimentation can ever prove me right; a single experiment can prove me wrong”

– Albert Einstein

WEE1 was a positive hit in the kinome siRNA screen, meaning that transfection with WEE1 siRNA would abrogate the G2 checkpoint. To test that the G2 checkpoint abrogation assay worked, the G2 checkpoint abrogation was first assayed in response to the WEE1 inhibitor MK1775. The results from the experiments with MK1775 were also useful since the effects on the G2 checkpoint with this inhibitor had not been tested previously in this research group.

5.1 Visualization of IR induced DNA damage in U2OS cells

In order to determine how the WEE1-inhibited cells were responding to IR, immunofluorescence images were taken of irradiated, WEE1 inhibited U2OS cells. The cells were antibody-stained to detect γ -H2AX and 53BP1, which are early components of the DSB induced ATM/ATR pathway and function as indicators of IR-induced DSBs. Fluorescent components; DAPI, Alexa 488 and Alexa 558 are binding to their respective epitopes; DAPI to DNA, Alexa 568 to 53BP1 and Alexa 488 to γ -H2AX. The fluorescence microscope and camera used to image both irradiated- and non-irradiated cells are described under **table 3.6**. The images of non-irradiated and irradiated cells are shown in **figures 5.1.1** and **5.1.2** respectively. The non-irradiated cells did not exhibit any significant foci formation of γ -H2AX and 53BP1, which indicates normal status; no significant DNA- damage in the cells. The images displaying γ -H2AX and 53BP1 is shown in **figures 5.1.1 (b)** and **(c)** respectively. **Figure 5.1.2** is displaying the irradiated cells, and it is shown clear evidence of 53BP1 and γ -H2AX foci formation, in **figures 5.1.2 (b)** and **(c)** respectively. **Figures 5.1.1 and 5.1.2(d)** are merged images of figures **(a-c)**, visualizing co localization of 53BP1 and γ -H2AX in yellow. **Figure 5.1.2(d)** is showing co localization of 53BP1 and γ -H2AX foci, indicating initiation of the IR-induced ATM/ATR pathway after 90 minutes. By comparing **figure 5.1.1** and **figure 5.1.2** it is clear that irradiation of WEE1

inhibited U2OS cells by 6Gy are causing DNA damage in form of DSBs, and are therefore initiating DNA damage checkpoints and repair.

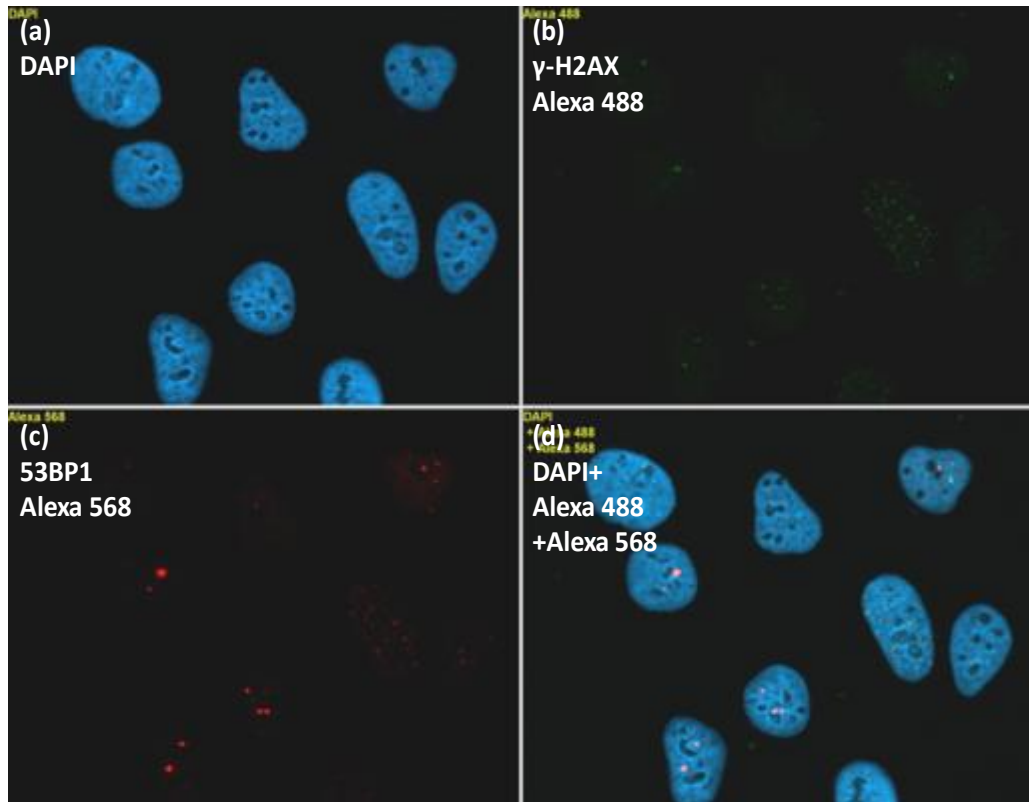


Figure 5.1.1(a-d) Immunofluorescence (IF) microscopy images of WEE1 inhibited U2OS cells: The cells were treated with 300nM MK 1775 for 105 minutes. Then they were stained with antibodies to detect γ -H2AX and 53BP1 and DAPI nuclear stain. Cells were pre-extracted removing everything but chromatin-bound components in the cell.

- (a) DAPI stain binds tightly to AT-rich regions in DNA, and Immunofluorescence reveals the DNA in the cell nucleus (blue). The black spots in the nucleuses are the nucleoli.**
- (b) Phosphorylated histone H2AX at serine 139 (γ -H2AX in green) flanking DNA double stranded breaks. γ -H2AX localized at nuclear foci represents DSBs.**
- (c) 53BP1 is shown in red, also indicating DNA damage. 53BP1 in DNA repair, are binding to γ -H2AX. 53BP1 localized at nuclear foci is representing DSBs.**
- (d) Merged images of (a) (b) and (c). Yellow spots indicate co localization of γ -H2AX and 53BP1**

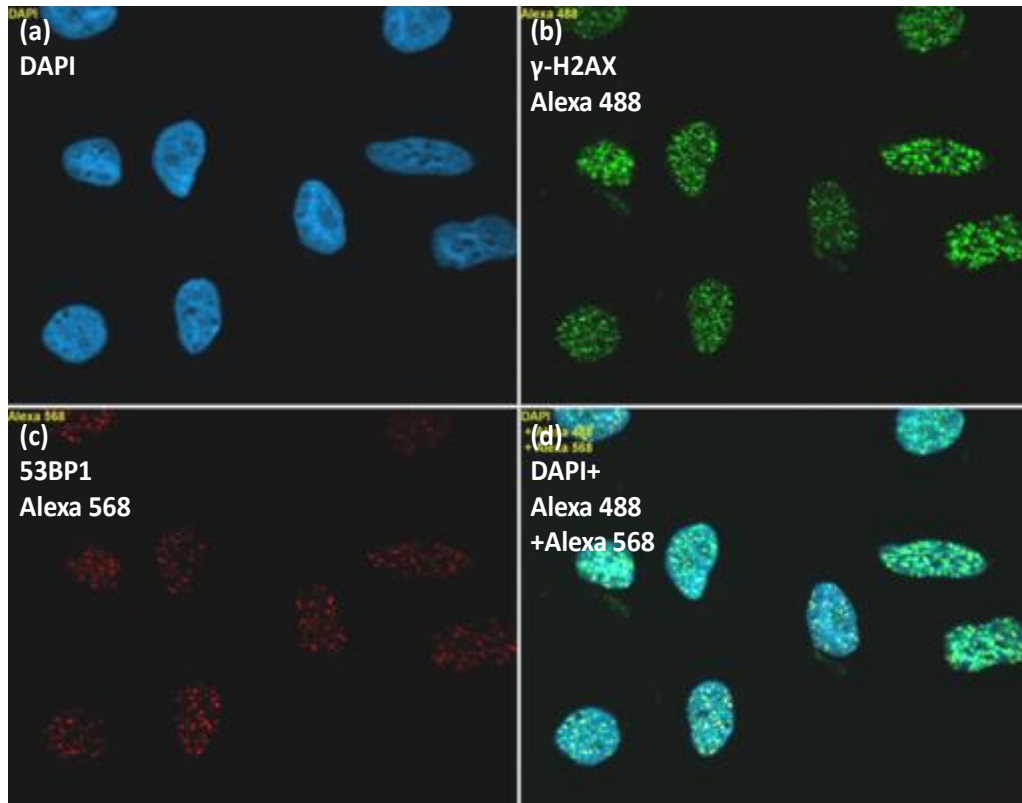


Figure 5.1.2(a-d) Immunofluorescence (IF) microscopy images of WEE1 inhibited U2OS cells: The cells were treated with 300nM MK 1775 for 105 minutes. MK 1775 was added 15 minutes previous to IR. Then they were stained with antibodies to detect γ -H2AX and 53BP1 and DAPI nuclear stain. Cells were pre-extracted removing everything but chromatin-bound components in the cell. (a) DAPI stain binds tightly to AT-rich regions in DNA, and Immunofluorescence reveals the DNA in the cell nucleus (blue). The black spots in the nucleuses are the nucleoli. (b) Phosphorylated histone H2AX at serine 139 (γ -H2AX in green) flanking DNA double stranded breaks. Localization of γ -H2AX at nuclear foci represents DBSs. (c) 53BP1 is shown in red, also indicating DNA damage. 53BP1 binds to γ -H2AX and functions in DNA repair. Localization of 53BP1 at nuclear foci represents DBSs. (d) Merged images of (a) (b) and (c). Yellow spots indicates co localization of γ -H2AX and 53BP1

5.2 Wee1 inhibition

5.2.1 Phenotypic analysis

To test the assay for checkpoint abrogation after irradiation, WEE1-inhibited cells were analyzed by flow cytometry following staining with γ -H2AX and H3-p antibodies. **Figure 5.2.1** is displaying the distribution of γ -H2AX- and H3-p-positive cells in a representative sample that were analyzed. The fraction of H3-p positive cells in the population is representative to the fraction of mitotic cells, also denoted as Mitotic Index (MI). The untreated, non-irradiated cells are showing a small population of mitotic cells, which represents the amount of cells present in mitosis at any time (**top left**). Untreated cells which are irradiated show no mitotic cells, which is due to effective G2 checkpoint arrest (**top middle**). However, irradiated cells treated with WEE1-inhibitor, display a higher mitotic index. This is indicating that the cells are escaping the G2 checkpoint, due to abrogation (**top right**). The lower row in **figure 5.2.1** is showing figures illustrating median γ -H2AX levels measured in the cell population against the DNA content. These figures give information about how the DNA damage in form of DSBs is distributed throughout the cell cycle, and the amount of DSBs. 300nM of MK1775 does not elevate median γ -H2AX levels, which indicates that it does not cause DNA damage in form of DSBs at 90 minutes post-IR. This analysis confirms what was seen in the Immunofluorescence Images, **Figures 5.1.1 and 5.1.2**. Raw data from flow cytometry analysis are shown in **Appendix B, tables B1-B3**.

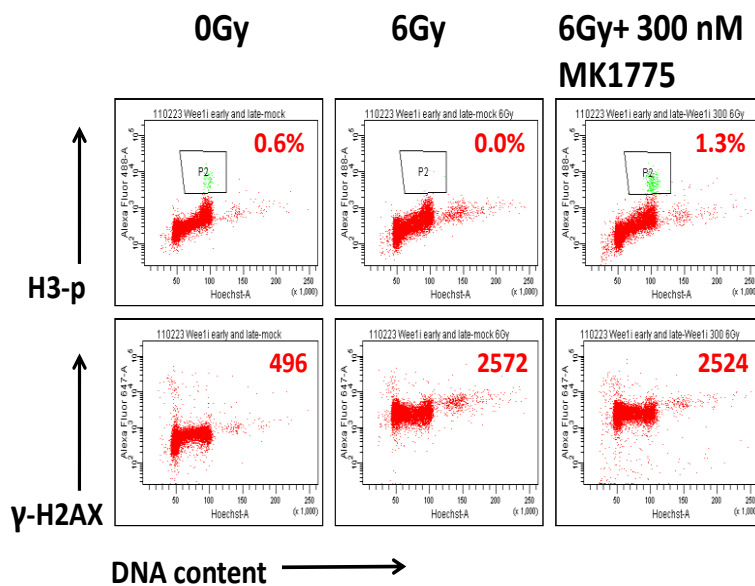


Figure 5.2.1 Phenotypic effect of WEE1 inhibition and radiation on cells: U2OS cells were treated with 300 nM of the WEE1 inhibitor MK1775 for 105 minutes. Irradiation was performed with 6Gy 15 minutes after inhibition. Next, the cells were stained for γ -H2AX and H3-p, and analyzed by Flow Cytometry. (Top row): H3-p positive cells as a function of DNA contents. (Top left): Un-irradiated cells. (Top middle): The irradiated cells, (Top right). Irradiated cells treated with 300nM WEE1 inhibitor. (Lower row): γ -H2AX as a function of DNA content is showed respectively for the different samples. The figure is showing results from a representative experiment.

5.2.2 Comparison of WEE1 inhibition in early- and late G2 checkpoint in U2OS cells

Inhibition of U2OS cells with MK 1775 was performed to investigate the effect of WEE1 inhibition of both the early and the late G2 checkpoint, shown in **figures 5.2.2(a) and (b) respectively**. Both experiments showed low or no MI at 6Gy in the non-inhibited cells, which is indicating a functioning G2 checkpoint. The experiments are also exhibiting the same trend with increasing MI with increasing concentration of MK1775, both in irradiated and in non-irradiated cells. The fraction of mitotic cells in the irradiated, MK1775 treated cells is indicating an abrogation of the G2 checkpoint induced by WEE1 inhibition. Inhibition with 300nM was found satisfactory for inhibition, both for the MI and for the level of cytotoxicity exerted by the inhibitor to the cells. For the results to be compared, the raw data had to be taken relative to the MI of untreated, un-irradiated cells and to the MI of nocodazole treated un-irradiated cells respectively.

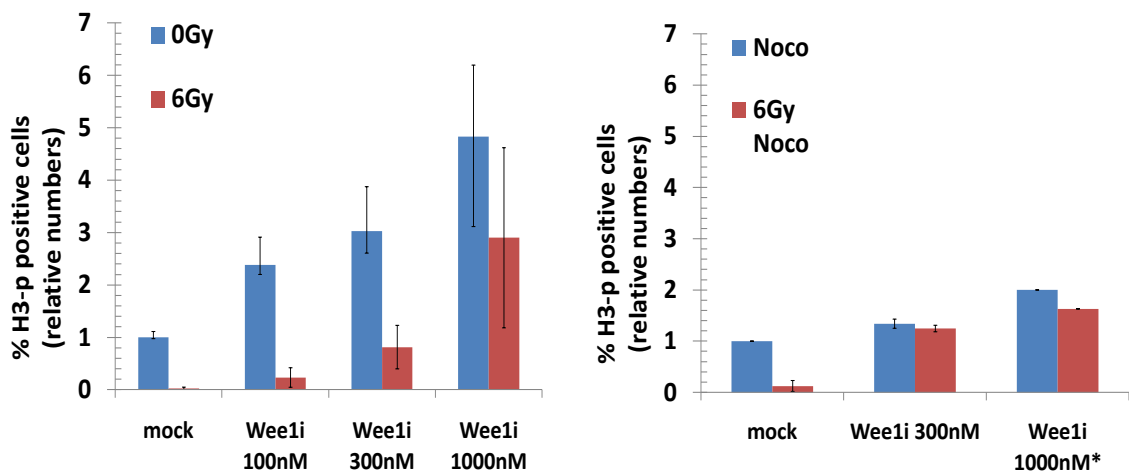


Figure 5.2.2(a, b) Early- versus late G2 checkpoint in U2OS cells: (a) Early G2 checkpoint (left). U2OS cells were treated with 100-, 300- and 1000 nM of the WEE1 inhibitor MK1775 for 105 minutes. Irradiation was performed with 6Gy, 15 minutes after inhibition. The cells were stained for H3-p and γ -H2AX and then analyzed by flow cytometry. Early checkpoint: Error bars indicate SEM (mock 0Gy n=5, mock 6Gy n=4, 100 nM 0- and 6Gy n=3, 300 nM 0Gy n=4 6Gy n=5, 1000nM both 0- and 6Gy n=4). (b) Late G2 checkpoint (right). U2OS cells were treated with 300 and 1000 nM of the WEE1 inhibitor MK1775 for 105 minutes. Irradiation was performed with 6Gy 15 minutes after inhibition. Nocodazole was added to the cells 2 hours after IR. Next, the cells were stained for H3-p and γ -H2AX and analyzed by flow cytometry. Late checkpoint: Error bars indicate SEM (n=2 except 1000nM where only one experiment was performed).

5.2.3 U2OS cells versus U2OSp53dd cells: Early G2 checkpoint

U2OS and U2OSp53dd cells were compared to see whether they both were affected similarly by WEE1 inhibition. This comparison was of interest because the U2OSp53dd cells were applied in the G2 checkpoint siRNA screen.

Inhibition of U2OS cells compared to the p53 deficient cells U2OSp53dd was also performed, shown in **figures 5.2.3 (a) and (b)** respectively. First, the early G2 checkpoint was investigated and the irradiated, untreated cells display no mitotic fraction, which indicates normal G2 checkpoint function. At inhibition with 300nM MK1775, both the non-irradiated and the irradiated cells were found to have an increased MI. The MI of the inhibited and irradiated cells is indicating an abrogation of the G2 checkpoint, induced by WEE1 inhibition, of about 2% in both cell lines. For the results to be compared, the raw data had to be taken relative to the MI of untreated, un-irradiated cells.

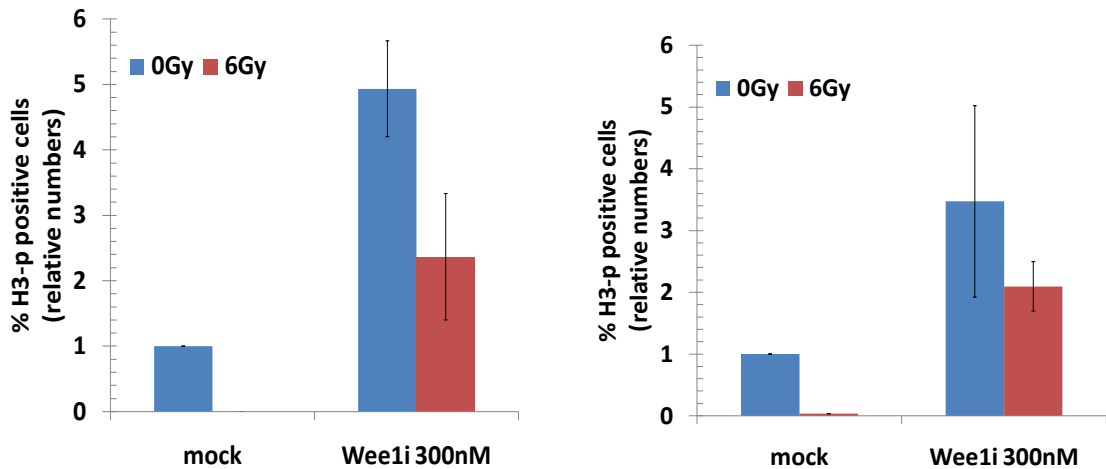


Figure 5.2.3 (a, b) U2OS- versus U2OSp53dd cells; Early checkpoint: (a): U2OS cells early G2 checkpoint (left) U2OS cells were treated with 300 of the WEE1 inhibitor MK1775 for 105 minutes. Irradiation was performed with 6Gy 15 minutes after inhibition. Next, the cells were stained for γ -H2AX and H3-p, and analyzed by Flow Cytometry. (b) U2OSp53dd cells early G2 checkpoint (right). U2OSp53dd cells were treated with 300 nM of the WEE1 inhibitor MK1775 for 105 minutes. Irradiation was performed with 6Gy 15 minutes after inhibition. Next, the cells were stained for γ -H2AX and H3-p, and analyzed by Flow Cytometry. Error bars indicate SEM, and n=2.

5.3. Validation of hits from phosphatome screen:

5.3.1 Optimization of transfection of esiRNAs

The effect of various silencing RNAs versus the WEE1-inhibitor MK1775 in irradiated cells, were tested in U2OSp53dd cells treated with nocodazole, shown in **figure 5.3.1(a)**. siCHK1 is the positive control. EsiRNAs were used in the experiments due to their promising low off target effects. The experiment indicated the effect of siCHK1 and MK1775 at the G2 checkpoint in irradiated cells. Also siSSH3 (the same siRNA for SSH3 as scored in the original siRNA screen) yielded an effect on the G2 checkpoint. EsiSSH3 did not seem to have any effect on checkpoint abrogation. **Figure 5.3.1(b)** is displaying the results from an experiment comparing the effect of siCHK1 with esiCHK1 in U2OSp53dd in order to use esiCHK1 as a positive control for further esiRNA transfection. In this experiment, the effects on abrogation of the G2 checkpoint were similar. Only one of these experiments was performed, so the MI can be varying, but the abrogating result of the checkpoint is clear. While the *phenotype* of the transfected cells are shown in **figures 5.3.1(a) and (b)**, is the *genotype* shown in **figure 5.3.1(c)** by a Western Blot. The blot shows that SSH3 is

down regulated to less than 25% of the normal levels by siSSH3, which does not correlates so well with the phenotype displaying a very low MI Down regulation of experiment with 50 % less RNA, and with normal condition shows a down regulation of CHK1 to less than 25% of normal levels. EsiCHK1 transfection with 50% fewer cells were down regulating CHK1 to about 25-50%. For siCHK1 transfection, CHK1 were almost completely down regulated. For the results to be compared, the raw data in **figure 5.3.2 (b)** had to be taken relative to the MI of untreated, un-irradiated cells and to the MI of nocodazole treated un-irradiated cells respectively.

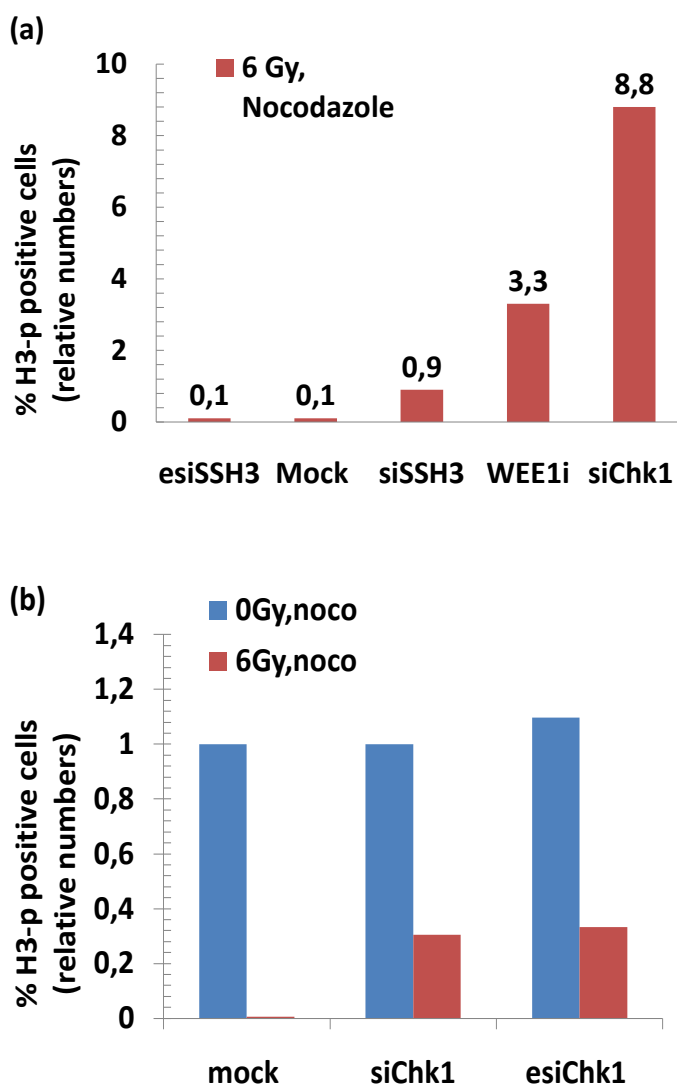


Figure 5.3.1 (a): Comparing esi- and siRNA transfection to WEE1 inhibition with MK1775. U2OSp53dd cells were transfected with esiSSH3, siSSH3 or siCHK1 for 48 hours (Oligofectamine transfection). Irradiation was performed with 6 Gy at 38 hours, and incubated for 2 hours. Then the cells were treated with nocodazole for 8 hours. The cells were stained for H3-p and γ -H2AX and analyzed by flow cytometry. For the WEE1 inhibition U2OS cells were treated with 300nM of the WEE1 inhibitor MK1775 for 105 minutes. Irradiation was performed with 6Gy, 15 minutes after inhibition. The cells were stained for H3-p and γ -H2AX and then analyzed by flow cytometry. (n=1).

Figure 5.3.1 (b) Comparing siCHK1 and esiCHK1 transfection. U2OSp53dd cells were transfected with siChk1 or esiCHK1 for 48 hours (Oligofectamine transfection). Irradiation was performed with 6 Gy at 38 hours, and incubated for 2 hours. Then the cells were treated with nocodazole for 8 hours. The cells were stained for H3-p and γ -H2AX and analyzed by flow cytometry. (n=1).

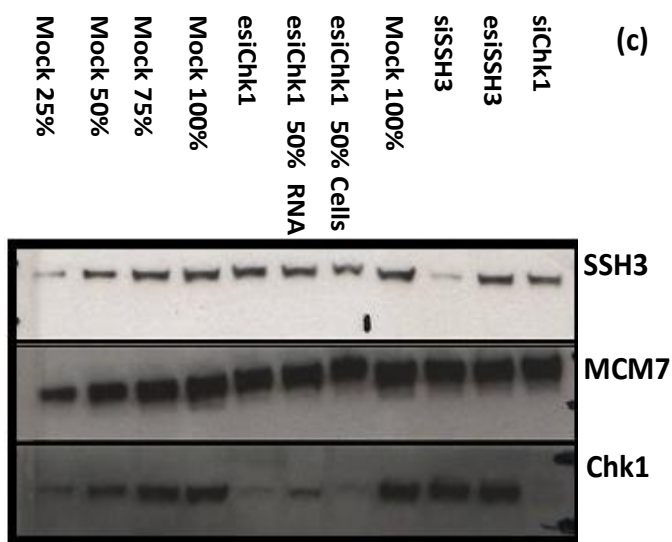


Figure 5.3.1(c): Protein levels of SSH3 andCHK1 after transfection. A Western Blot is shown in this figure and is displaying the genotype of the cells transfected with siCHK1, siSSH3, esiCHK1 and esiSSH3. MCM7 is the loading control. The membrane obtained from the Western Blotting was antibody-stained for SSH3, CHK1 and MCM7.

5.3.2 Optimization of transfection reagents: Oligofectamine compared to Effectene.

From **figure 5.3.1(c)** it is shown that the esiSSH3 did not downregulate SSH3 in any significant way . SSH3 is one of the hits from the siRNA screen prior to this project ,and therefore it was tried to optimize the transfection conditions for esiRNAs. Two different transfection reagents were compared ; Oligofectamine and Effectene in addition to two different timepoints for fixing of cells post-transfection. CHK1 and SSH3 were the targets for downregulation , and all esiCHK1 samples were found to downregulate better with Effectene than Oligofectamine.The 48 hour timepoint esiCHK1 with effectene were found to downregulate CHK1 almost completely . However, SSH3 did not down regulate significantly. It was used an old batch of esiSSH3 for this transfection.The results are shown in **figure 5.3.2** and the conditions are explained more in detail in **table 5.3.1**.

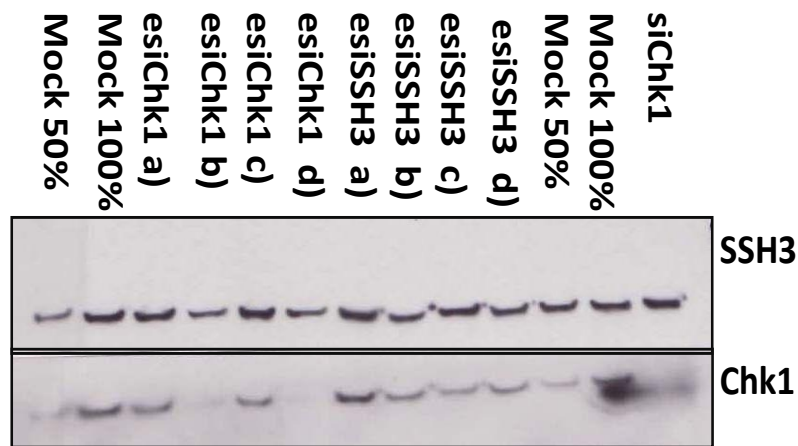


Figure 5.3.2 Oligofectamine- versus effectene transfection: U2OSp53dd cells were transfected with esiCHK1 and esiSSH3. The respective conditions a), b), c) and d) for each sample is shown in table 5.3.1. The cells were harvested and fixed at 48- and 72 hours post-transfection. The samples were then analyzed by Western Blotting, antibody-staining for SSH3 and CHK1.

Table 5.3.1: Showing conditions for transfection of esiCHK1 and esiSSH3. Volumes are per 35mm dish, with 1×10^5 cells plated.

Condition	Transfection reagent	Fixing of cells [Hours post transfection]	esiRNA [μ l]
a	Oligofectamine	48	10
b	Effectene	48	20
c	Oligofectamine	72	10
d	Effectene	72	20

5.3.3 Optimization of effectene as a transfection reagent for esiRNAs

Finding that Effectene transfection agent has a good effect on esiRNA transfection, lead to further optimization of this process. Different conditions for esiRNA transfection were performed with esiSSH3, and the results from the Western Blotting are shown in figure 5.3.3. The different conditions are shown in detail in table 5.3.2. Again two time points for cell-fixing post-transfection was tried out, together with all the transfection conditions of esiSSH3. A new batch of esiSSH3 was used, and down regulation to less than 50 % of SSH3 was shown at all conditions. However, the condition c) indicated to have the best effect in both time points. The cell morphology was checked in a microscope at 48 hours and at 72

hours. At 48 hours, esiSSH3 cells condition a) and c) had some vacuole formation and altered morphology due to cytotoxicity of Effectene. EsiSSH3 transfected cells and condition c) still looked healthier than the ones with condition a). The cells transfected with esiSSH3 and condition b) looked the healthiest, but also gave a lower effect of down regulation. At 72 hours transfection, the esiSSH3 transfected samples were displaying the following characteristics; condition a) had many vacuoles, but healthy, b) had many vacuoles and many dead cells. For esiSSH3, c) most cells were dead or dying, and had detached. This may be the reason for why the SSH3 levels were so low in this sample. Thus, condition c) might be highly cytotoxic at 72 hours transfection. This might be due to the high Effectene: esiRNA concentration ratio at condition c). For further esiRNA transfection experiments Effectene with condition c) and 48 hours post-transfection-fixing were chosen.

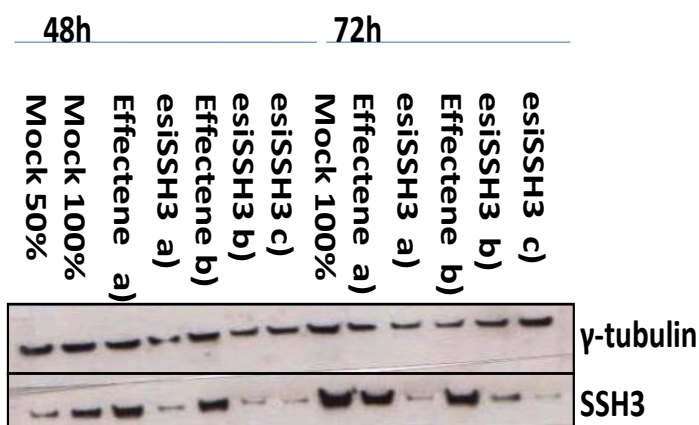


Figure 5.3.3 Optimization of Effectene as a transfection agent: Western Blot of esiSSH3 transfected U2OSp53dd cells .The conditions a), b) and c) were performed.U2OSp53dd cells were transfected with esiSSH3 or just Effectene for 48 and 72hours. The cells were antibody-stained for SSH3 and γ-tubulin and analyzed by Western Blotting. γ-tubulin is the loading control.

Table 5.3.2: Showing transfection conditions for esiSSH3- transfection of U2OSp53dd cells and optimization of Effectene. The volumes are according to a 35mm dish, with 1×10^5 cells plated.

Condition	esiRNA [μl]	Enhancer [μl]	Effectene [μl]
a	10	3,2	10
b	10	3,2	5
c	5	3,2	10

5.3.4 Preliminary results on validation of phosphatome-screen hits

Preliminary results from esiRNA transfection of U2OSp53dd cells for candidate hits from the phosphatome screen is shown in **figure 5.3.4**. So far, esiSSH3 and esiPTPN7 have been applied. The method of transfection is based on previous experiments; Effectene transfection with condition c), showed in **table 5.3.2**, with cell- fixing 48 hours post-transfection. From this experiment only the positive control, esiCHK1, showed an abrogation of the G2 checkpoint at 6Gy. This experiment needs more testing for validation or rejection of any of the hits.

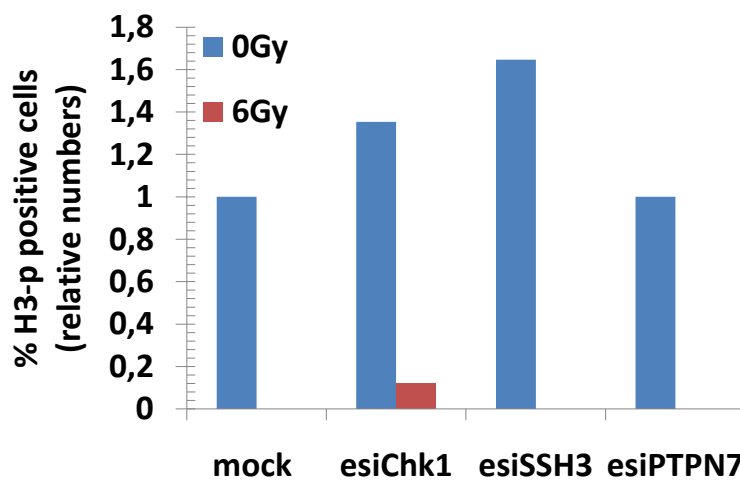


Figure 5.3.4 Preliminary results from validation of hits from the siRNA screen: U2OSp53dd cells were transfected with the following esiRNAs; esiCHK1, esiSSH3, esiDUSP16 and esiPTPN7 by Effectene transfection reagent and condition c) from table 5.3.2 for 48hours. Irradiation was performed with 6 Gy after 38 hours of transfection, and then incubated for 2 hours. Afterwards, the samples were treated with nocodazole for 8 hours. The cells were stained for H3-p and γ -H2AX and analyzed by flow cytometry. (n=1).

6. Discussion

6.1 Confirming the siRNA assay

6.1.1 WEE1 inhibition

WEE1 was a positive hit in the kinome siRNA screen meaning that transfection with WEE1 siRNA would abrogate the G2 checkpoint[55]. To test that the G2 checkpoint abrogation assay worked, the G2 checkpoint abrogation was first assayed in response to the WEE1 inhibitor MK1775. The results from the experiments with MK1775 were also useful since the effects on the G2 checkpoint had not been tested previously in this research group. The results from this project are indicating that WEE1inhibition of U2OS cells could abrogate both the early and late G2 checkpoint. Different concentrations for the inhibitor were tested, and the mitotic index (MI) for irradiated samples was increasing in a dose-dependent matter. As a compromise between G2 abrogation-effect and cytotoxicity, 300nM MK1775 were the chosen condition for further experiments. MK1775 inhibition alone is found to cause minimal cytotoxicity at 300nM., which is also shown earlier in this project, in **figure 5.1.1** [41]. It is of importance that the cytotoxicity of WEE1 inhibitor in monotreatment is low. By specifically attacking cancer cells with a defective G1 damage checkpoint, the normal- functioning cells will be spared to a greater extent. In the literature, 300nM of MK1775 in combination with IR was found to inhibit WEE1 in U2OS cells and cause an abrogation of the G2 checkpoint leading to mitotic catastrophe and cell death [41] .

From the comparison of the early and the late G2 checkpoint in U2OS cells, it seems like the WEE1 inhibitor more efficiently abrogated the late G2 checkpoint compared to the early G2 checkpoint. The early- and the late G2 checkpoints are known to have different molecular mechanisms, which might be influencing on how they react to WEE1 inhibition[34].

However, the error bars in **figure 5.2.2(a)** are very large for all the irradiated samples treated with MK1775. An explanation for this could be an unstable MK1775 inhibitor, due to repeated freezing and thawing cycles for every experiment. One of the experiments is showing a greater MI than the others. This is affecting the SEM, and resulting in a larger error bar. Another source of uncertainty, is the low number of repetitions (n=2) of these experiments.

U2OSp53dd cells were used in the siRNA screen prior to this project, so the MK1775 also needed to be tested for this cell line in order to relate this project to the siRNA screen. In addition, it is important to confirm that the effect of WEE1 inhibition is p53 independent, since many cancers arise from deletions or mutation in the P53 gene. The experiments comparing the effect of MK1775 at 300nM in U2OS- contra U2OSp53dd gave results that implied that the MI of MK1775 inhibition of the two cell lines was similar. At 6 Gy the average MI were found to 2.4 and 2.1 for U2OS- and U2OSp53dd cells respectively.

It was performed n=2 parallels of this experiment, so to reduce the uncertainties, more experiments should be performed. To roughly indicate the reproducibility of the results it was chose to calculate the error bars based on the two experiments. To determine the standard deviation and SEMs more precisely, more repetitions are needed. Anyhow, MK1775 was found to cause an abrogation in the G2 checkpoint for both cell lines in these experiments. In the literature, MK1775 inhibition was not showed to sensitize p53 wild type cells, in three different colon cancer cell lines when treated with the DNA damaging agent, 5-fluorouracil[41].

6.1.2 Current research for WEE1 inhibition

The abrogation of the G2 checkpoint by WEE1 inhibition with MK1775 was found to be effective, confirming that the G2 checkpoint abrogation assay worked. It was expected that WEE1 inhibition would work since MK1775 is well tested for. MK1775 in combination with IR have been investigated in preclinical studies. Subsequently, it was found that the combination was radio sensitizing p53 deficient human tumor xenografts (p53 mutant H1299 and p53 null) but not the p53 wild type ([wt] A549).[56] Furthermore, MK1775 is also in phase I /II in clinical trials, by combination treatment with the DNA damaging agents; gemcitabine, 5-fluoruracil, and cisplatin[41].The other WEE1 inhibitors of significance PD0166285 and PD0407824, have not been tested in patients[42].The

PD0166285, is known to radio- sensitize p53 deficient ovarian cancer cells to IR[57].In addition, it was recently found that PD0166285 could sensitize the human osteosarcoma cell lines; MG-63, U2OS and SaOS-2 in the presence of IR. However, MK 1775 is a pyrazolo-pyrimidine derivative that is a potent and more selective inhibitor of WEE1, and known to be highly specific against Myt, (**figure 2.9**)[42]. Compared to other WEE1 inhibitors like the PD0166285, MK1775 is displaying less cytotoxicity, which is most likely due to its specificity[1].

6.1.3 Future goals for G2/M checkpoint abrogation studies

G2 checkpoint abrogation strategy is *selective* in the sense that it *selectively* targets cells that depends on G2-checkpoint arrest solely. Thus, the p53-deficient tumor cells are forced into mitotic catastrophe, while the p53 efficient cells can cope with the damage in G1 phase[42].In this sense, the beneficial traits that cancer cells' exhibit for growth and proliferation are exploited to combat them.

The best therapeutic target to G2 checkpoint abrogation is still unclear. It might be some of the known G2/M regulators such as; ATR, CHK1, MYT1, Hsp90, PP2A, WEE1, or other unknown G2/M regulators yet to be found[42]. Combinations of these are under consideration for future work together with improving the selectivity of the WEE1inhibitors. MK1775 is strictly specific, but increased selectivity would give an even lower cytotoxic profile. A reproducible, specific and highly efficient target- engagement is desired. Moreover, the optimal timing for applying DNA damaging agents such IR and with subsequent WEE1inhibtion, is also of importance. [42]

Combination treatment of DNA damaging agents and WEE1 inhibition is justifying the present safety- and efficiency expectancies, but has a great developing potential.

[42]

6.2 Validation of hits from the siRNA screen

6.2.1 EsiRNA transfection

With the confirmation of the assay, validation experiments of positive hits from the siRNA screen could be performed. WEE1 inhibition of U2OSp53dd cells was compared to transfection of esiSSH3 and siSSH3. WEE1 inhibition gave the highest MI, except for the positive control siCHK1. The first results indicated that transfection with the siSSH3 oligo that scored in the original screen lead to abrogation of the checkpoint to some extent, but not with esiSSH3. This is shown in **figure 5.3.1(a, b)** The results from the Western Blotting, shown in **figure 5.3(c)**, confirmed this by displaying a down regulation of SSH3 by siSSH3, but not by esiSSH3.

Comparing siCHK1- and esiCHK1 transfection lead to abrogation of the G2 checkpoint and clear down regulation of the CHK1 protein. On the basis of these results, esiCHK1 were chosen as a positive control for esiRNA transfections.

The ideal transfection conditions are obtaining highest possible transfection efficiency, while the toxicity is at a minimum. This can be described as the earliest time-point showing the highest protein level of down regulation of the target. These conditions are varying with the knock-down kinetics of the certain target[4]. Thus, two time-points of transfection were included to the optimization experiments.

6.2.2 Optimization of esiRNA transfection

EsiRNA transfection optimization was performed by comparing results from transfections of U2OSp53dd cells with the transfection reagents Oligofectamine and Effectene. The results from these experiments, shown in **figure 5.3.2**, demonstrated that the positive control, esiCHK1, was more efficiently down regulated with Effectene than Oligofectamine. SSH3 was not found to be down regulated by esiSSH3 in any significant way in any samples. The blot is missing a loading control to measure the amount of proteins loaded to the wells on the gel. Varying amounts of protein added to the test, can give un-proportional occurrence in the protein bands. However, the protein lysates were analyzed for protein quantification prior to western blotting, giving more reliable results

due to more equal loading on the gel. This is shown by the relatively stable amounts of SSH3 in the bands throughout the blot.

For further optimization of esiRNA transfection with Effectene as a transfection reagent, different concentrations of Effectene and esiRNA were tried out. Effectene is the recommended transfection reagent for U2OS cells by The Max Planck Institute of Molecular Cell Biology and Genetics. [53] All the conditions had higher effectene concentrations than from the ones in **figure 5.3.2**, trying to achieve down regulation also of SSH3 by the esiSSH3. Transfection with esiSSH3 and Effectene with condition c) were found to give the smallest protein bands for SSH3 at both 48- and 72 hours transfection. The blot is shown in **figure 5.3.3**. The 72 hours time point exerted massive cytotoxicity, with mostly detached, dead or dying cells. Detached cells are washed off before cell fixing (**section 4.11**) and are therefore most likely to be responsible for the low protein yield on the band. For this reason, the 72 hour transfection was excluded. For further work the transfection with condition c) and 48 hours was chosen. This condition has also the highest Effectene: esiRNA ratio.

Comparing **figure 5.3.2** and **5.3.3** are showing down regulation of SS3 in the last mentioned figure, but not in the first. In the first experiment it was used esiSSH3 from an old batch and in the second, a new batch of esiSSH3 was applied giving different results. Reason for the distinct results in the two experiments may be an unstable esiSSH3, due to repeated freezing and thawing cycles, or that the conditions tried in the first experiment were not sufficient to down regulate the protein.

6.2.3 Validation experiments of esiSSH3 and PTPN7

From the hits from the phosphatome G2 checkpoint siRNA screen, shown in **table 2.1**, protein phosphatase Slingshot homolog 3 (SSH3) and protein tyrosine phosphatase, non-receptor type 7 (PTPN7) were chosen for validation in this project. SSH3 was chosen because it is known to be phosphorylated by ATM/ATR, and PTPN7 because it works to suppress MAP kinase activities [58, 59]. Both ATM/ATR and MAP kinases have been implicated in DNA damage responses and cell cycle progression in previous studies. However, the preliminary results from **figure 5.3.4** show no abrogation in the G2 checkpoint, neither by esiSSH3 nor esiPTPN7. It is not known whether the PTPN7 protein levels were down regulated or not. Western Blotting analysis of the protein lysates from the esiPTPN7 samples would have given an indication of the protein-level status after transfection with esiPTPN7. However, Western blotting for PTPN7 could not be performed because functional PTPN7 antibodies are not available [60]. **Figure 5.3.3** is by western blotting, showing down regulation of SSH3 by esiSSH3 transfection. siRNAs are known to cause more off-target effects than esiRNA, and one explanation for the G2-checkpoint abrogation by siSSH3, could be off target effects. If that is the case, then SSH3 is either not down regulated enough to cause a phenotypic abrogation, or it is not a real hit in the screen.

Anyhow, the siRNA – and the esiRNA-transfections were only performed once, so the statistic uncertainties are high. The abrogation by siSSH3 can be due to statistical variance or other errors. The experiments need more testing in order to either reject or validate the hits from the siRNA screen.

6.2.4 Comparison to other G2 checkpoint siRNA screens

High throughput large-scale G2 checkpoint siRNA screens have not been reported before June 2011. On June 3rd the screen setup by Randi Syljuåsens research group, using the kinome and DNA repair factor libraries, were published[60]. On June 10th an independent G2 checkpoint screen was published by another group[60]. The screen from the other group was performed in U2OS with a whole genome Dharmacon library with different siRNA oligos than in the first screen. Neither PTPN7 nor SSH3 scored in the full genome screen. This fact can support the absence of G2 abrogation in the esiSSH3 and esiPTPN7 – transfection experiments. Interestingly, 2 of the hits from the whole- genome screen

were also found in the phosphatome screen[60].These correlating hits from both screens were protein phosphatase 2C, magnesium-dependent, catalytic subunit (PPM2C) and dual specificity phosphatase 16 (DUSP16). DUSP16 is involved in inactivating the stress-activated p38 and JNK MAPkinases[60].

6.2.5 Future work

In the whole-genome screen both DUSP16 and PPM2C scored weakly. In the phosphatome screen, both of these genes scored with only one siRNA, and their MI were 3,694 and 2,365 respectively. The candidate hits and their respective scores are found the **table A1** in **appendix A**.

PP2CB (PP2A) scored relatively low in the phosphatome screen, despite its published role in the IR induced G2 checkpoint. This might give hope for other hits with a lower score. A study demonstrated that specific siRNA inhibition of PP2A abrogated the IR-induced activation of ATR, CHK1 kinases and the phosphorylation of CDC2-Tyr15 residues[61].he expression of PP2CB has also been found to be significantly reduced in prostate carcinoma[62].Thus, PP2A scored only with one siRNA and the MI was 1,325. The MIs for PPM2Cand DUSP16 were both higher than the one for PP2A. This might imply that DUSP16 and PPM2C are worth investigating further for their role in the G2/M checkpoint. PTPN7 and SSH3 had MI scores at 2,692 and 3,439 respectively in the phosphatome siRNA screen. They were not found as hits in the whole-genome siRNA screen , and were not showing any abrogation of the G2 checkpoint in the experiments with esiRNA transfection. This might imply that their role as hits in the phosphatome screen were due to off target effects. However, no conclusion can be drawn before more validation experiments are done.

7. Conclusion

"The open mind never acts: when we have done our utmost to arrive at a reasonable conclusion, we still - must close our minds for the moment with a snap, and act dogmatically on our conclusions."

-George Bernard Shaw

It was found that the early- and the late G2 checkpoint were abrogated by WEE1 inhibition by the small molecule inhibitor MK1775 in U2OS cells irradiated with 6Gy. U2OS and the U2OSp53dd cells both had a similar level of G2 checkpoint abrogation when treated with MK1775.

The second part of the project was validation of candidate hits from the phosphatome screen in U2OSp53dd cells. To validate the hits transfection with esiRNA was used to down regulate candidate hits. EsiRNA was used because it is considered to give less off target effects than siRNAs. Following experiments to optimize the transfection conditions for esiRNA, Effectene was chosen over Oligofectamine as the preferred transfection reagent. Among the candidate hits from the phosphatome G2 checkpoint siRNA screen, protein phosphatase Slingshot homolog 3 (SSH3) and protein tyrosine phosphatase, non-receptor type 7 (PTPN7) were chosen for validation. However, the preliminary results show no abrogation in the G2 checkpoint in irradiated cells, neither by esiSSH3 nor esiPTPN7. Thus, SSH3 and PTPN7 were most likely false hits in our screen, probably due to off target effects. These results are consistent with the results of a recently published G2 checkpoint siRNA screen targeting the whole genome, where SSH3 and PTPN7 were not among the positive hits.

8. References

1. PosthumaDeBoer, J., et al., *WEE1 inhibition sensitizes osteosarcoma to radiotherapy*. BMC Cancer, 2011. **11**(1): p. 156.
2. Darling, T.W.o.D. The Worlds of David Darling [cited 2011 02.07]; Available from: http://www.daviddarling.info/encyclopedia/C/cell_cycle.html.
3. Cooper., G.M., *The Cell: A Molecular Approach*. 2nd edition ed. 2000, Boston University.
4. Theis, M. and F. Buchholz, *High-throughput RNAi screening in mammalian cells with esiRNAs*. Methods, 2011. **53**(4): p. 424-429.
5. gsbharaj. *CELL BIOLOGY* 78. 2011 [cited 2011 03.07]; Available from: http://hubpages.com/hub/cell_biology.
6. Nobelprize.org. *Physiology or Medicine for 2001 - Press Release*. [cited 2011 4 Jul]; Available from: http://nobelprize.org/nobel_prizes/medicine/laureates/2001/press.html.
7. Seiichi Ishida, E.H., 1 Harry Zuzan, 2 Rainer Spang, 2 Gustavo Leone, 1† Mike West, 2 and Joseph R. Nevins1*, *Role for E2F in Control of Both DNA Replication and Mitotic Functions as Revealed from DNA Microarray Analysis*. Mol Cell Biol., 2001((14)): p. 4684–4699. .
8. Gustavo Leone, 3 James DeGregori, 1,3,4 Zhen Yan, 2 Laszlo Jakoi, 1 Seiichi Ishida, 1 R. Sanders Williams, 2 and Joseph R. Nevins1,5, *E2F3 activity is regulated during the cell cycle and is required for the induction of S phase*. Genes Dev 1998. **12**((14)): p. 2120–2130. .
9. Harrison, M., A. Adon, and H. Saavedra, *The G1 phase Cdks regulate the centrosome cycle and mediate oncogene-dependent centrosome amplification*. Cell Division, 2011. **6**(1): p. 2.
10. Meloche, S. and J. Pouyssegur, *The ERK1//2 mitogen-activated protein kinase pathway as a master regulator of the G1- to S-phase transition*. Oncogene, 0000. **26**(22): p. 3227-3239.
11. Watkins, T. *Cell Division - Eukaryotic cell division*. 2011; Available from: <http://science.jrank.org/pages/1322/Cell-Division.html>.
12. Kimball, J.W., *The Cell Cycle*. 2011.
13. Hochegger, H., Takeda, S., & Hunt, T., *Cyclin-dependent kinases and cell-cycle transitions: does one fit all?* Nature Reviews Molecular Cell Biology 2008. **9**: p. 910-916
14. Online, M.R.a.M.P. *Generalized Eukaryotic Cell*. 2008; Available from: <http://mcat-review.org/generalized-eukaryotic-cell.php>.
15. *Mutation and Cancer*. 2010 [cited 2011 04.07]; Available from: <http://www.cancerquest.org/mutation-and-cancer>.
16. Lodish H, B.A., Zipursky SL, et al., *Molecular Cell Biology*. 2000., W. H. Freeman and Company.
17. Sung, P. and H. Klein, *Mechanism of homologous recombination: mediators and helicases take on regulatory functions*. Nat Rev Mol Cell Biol, 2006. **7**(10): p. 739-750.
18. Kimball, J.W. *Kimball's Biology Pages*. 12 March 2011 Available from: http://users.rcn.com/jkimball.ma.ultranet/BiologyPages/D/DNArepair.html#The_Generation_of_Antibody_Diversity.
19. Raynard, S., H. Niu, and P. Sung, *DNA double-strand break processing: the beginning of the end*. Genes & Development, 2008. **22**(21): p. 2903-2907.
20. Allen, C., C.A. Miller, and J.A. Nickoloff, *The mutagenic potential of a single DNA double-strand break in a mammalian chromosome is not influenced by transcription*. DNA Repair, 2003. **2**(10): p. 1147-1156.

21. Tacitus, C., *The histories and the annals*. 1937, Harvard University Press: Cambridge. p. 4 v.
22. Kimball, J.W. *Apoptosis ;Kimball's Biology Pages*. 2011 7 February 2011 [cited 2011 04.07]; Available from: <http://users.rcn.com/jkimball.ma.ultranet/BiologyPages/A/Apoptosis.html>.
23. Fagagna, F.d.A.d., et al., *A DNA damage checkpoint response in telomere-initiated senescence*. *Nature*, 2003. **426**(6963): p. 194-198.
24. Ljungman, M., *Activation of DNA damage signaling*. *Mutation Research/Fundamental and Molecular Mechanisms of Mutagenesis*, 2005. **577**(1-2): p. 203-216.
25. R&D Systems, I. *DNA Damage Response*. 2003 [cited 2011 04.07]; Available from: http://www.rndsystems.com/mini_review_detail_objectname_MR03_DNADamageResponse.aspx.
26. Kastan, M.B., *DNA Damage Responses: Cancer and Beyond Have we learned enough to design new therapies or prevention approaches?* . *The Scientist* 2005. **19**((19)).
27. Deckbar, D., P.A. Jeggo, and M. Löbrich, *Understanding the limitations of radiation-induced cell cycle checkpoints*. *Critical Reviews in Biochemistry and Molecular Biology*. **0**(0): p. 1-13.
28. Cell Signaling Technology, I. *Cell Cycle Control: G1/S Checkpoint*. 2010 [cited 2011 0407]; Available from: http://www.cellsignal.com/reference/pathway/Cell_Cycle_G1S.html.
29. Alberts B, J.A., Lewis J, et al., *Molecular Biology of the Cell*. . 2002.
30. Bartek, J. and J. Lukas, *Pathways governing G1/S transition and their response to DNA damage*. *FEBS Letters*, 2001. **490**(3): p. 117-122.
31. Shapiro, G.I., *Cyclin-Dependent Kinase Pathways As Targets for Cancer Treatment*. *Journal of Clinical Oncology*, 2006. **24**(11): p. 1770-1783.
32. Focosi, D. *G2/M DNA damage checkpoint*. 2009 [cited 2011 0407]; Available from: http://www6.ufrgs.br/favet/imunovet/molecular_immunology/g2mmap.html.
33. *9 The Cell Cycle*. [cited 2011 0407]; Available from: <http://kc.njnu.edu.cn/swxbx/shuangyu/9.htm>.
34. Xu, B., et al., *Two Molecularly Distinct G2/M Checkpoints Are Induced by Ionizing Irradiation*. *Mol. Cell. Biol.*, 2002. **22**(4): p. 1049-1059.
35. Edited by Albert Van der Kogel, M.J., *Basic Chemical Radiobiology Chapter 2* 4th edition ed. 2010: Oxford University Press.
36. Cahill, D.P., et al., *Genetic instability and darwinian selection in tumours*. *Trends in Cell Biology*, 1999. **9**(12): p. M57-M60.
37. Fang, Y.-Z., S. Yang, and G. Wu, *Free radicals, antioxidants, and nutrition*. *Nutrition (Burbank, Los Angeles County, Calif.)*, 2002. **18**(10): p. 872-879.
38. Bucher, N. and C.D. Britten, *G2 checkpoint abrogation and checkpoint kinase-1 targeting in the treatment of cancer*. *Br J Cancer*, 2008. **98**(3): p. 523-528.
39. Castedo, M., et al., *Mitotic catastrophe constitutes a special case of apoptosis whose suppression entails aneuploidy*. *Oncogene*, 2004. **23**(25): p. 4362-4370.
40. De Witt Hamer, P.C., et al., *WEE1 kinase targeting combined with DNA damaging cancer therapy catalyzes mitotic catastrophe*. *Clin Cancer Res*, 2011.
41. Hirai, H., et al., *MK-1775, a small molecule Wee1 inhibitor, enhances anti-tumor efficacy of various DNA-damaging agents, including 5-fluorouracil*. *Cancer Biology & Therapy*, 2010. **9**(7): p. 514-522.
42. De Witt Hamer, P.C., et al., *WEE1 Kinase Targeting Combined with DNA-Damaging Cancer Therapy Catalyzes Mitotic Catastrophe*. *Clinical Cancer Research*, 2011.

43. Boutros, R., V. Lobjois, and B. Ducommun, *CDC25 phosphatases in cancer cells: key players? Good targets?* *Nat Rev Cancer*, 2007. **7**(7): p. 495-507.
44. Link, G. *What is RNAi and siRNA?* [cited 2011 0407]; Available from: <http://www.genelink.com/sirna/RNAiwhatis.asp>.
45. Nobelprize.org. "Advanced Information: The 2006 Nobel Prize in Physiology or Medicine." [cited 2011 0407]; Available from: http://nobelprize.org/nobel_prizes/medicine/laureates/2006/adv.html.
46. Aagaard, L. and J.J. Rossi, *RNAi therapeutics: Principles, prospects and challenges*. *Advanced Drug Delivery Reviews*, 2007. **59**(2-3): p. 75-86.
47. N Manjunath, D.M.D., *Advances in Synthetic siRNA Delivery*. *Discovery Medicine*, 2010.
48. Qiu, S., C.M. Adema, and T. Lane, *A computational study of off-target effects of RNA interference*. *Nucleic Acids Research*, 2005. **33**(6): p. 1834-1847.
49. Watts, J.K., G.F. Deleavey, and M.J. Damha, *Chemically modified siRNA: tools and applications*. *Drug Discovery Today*, 2008. **13**(19-20): p. 842-855.
50. Hesketh, C. *siRNA delivery methods*. 2009 [cited 2011 0407]; Available from: <http://www.ionchannels.org/content.php?contentid=8>.
51. Watts, J.K. and D.R. Corey, *Clinical status of duplex RNA*. *Bioorganic & Medicinal Chemistry Letters*, 2010. **20**(11): p. 3203-3207.
52. Co, S.-A. *esiRNA/esiFlex*. [cited 2011 0407]; Available from: <http://www.sigmaaldrich.com/life-science/functional-genomics-and-rnai/mission-esirna.html>.
53. Genetics, M.P.I.o.M.C.B.a. *esiRNA Homepage* [cited 2011 0407]; Available from: <http://www.mpi-cbg.de/esiRNA/kdspecificity.html>
<http://www.mpi-cbg.de/esiRNA/protocols.html>.
54. QIAGEN. *Effectene Transfection Reagent Handbook - English (PDF)*. 2002 [cited 2011 0407]; Available from: <http://www.qiagen.com/literature/render.aspx?id=380>.
55. Menzel, T., et al., *A genetic screen identifies BRCA2 and PALB2 as key regulators of G2 checkpoint maintenance*. *EMBO Rep*, 2011. **12**(7): p. 705-712.
56. K. Mason, J.P., C. Ware, H. Hirai, P. Strack, S. D. Shumway, K. Ang, T. A. Buchholz, L. Milas, C. A. Buser; University of Texas M. D. Anderson Cancer Center, Houston, TX; Merck & Co., Inc., Boston, MA; Tsukuba Research Institute, Ibaraki, Japan; Merck Research Laboratories, Boston, MA; Merck & Co., Inc., North Wales, PA *Preclinical in vivo evaluation of a novel treatment strategy combining a Wee1 inhibitor with radiotherapy*. *J Clin Oncol* 28:15s, 2010 (suppl; abstr 10596), 2010.
57. Wang, Y., et al., *Radiosensitization of p53 Mutant Cells by PD0166285, a Novel G2 Checkpoint Abrogator*. *Cancer Research*, 2001. **61**(22): p. 8211-8217.
58. Matsuoka, S., et al., *ATM and ATR Substrate Analysis Reveals Extensive Protein Networks Responsive to DNA Damage*. *Science*, 2007. **316**(5828): p. 1160-1166.
59. Science, W.I.o. *Gene cards; protein tyrosine phosphatase, non-receptor type 7*. [cited 2011 0407]; Available from: <http://www.genecards.org/cgi-bin/carddisp.pl?gene=PTPN7>.
60. Cotta-Ramusino, C., et al., *A DNA Damage Response Screen Identifies RHINO, a 9-1-1 and TopBP1 Interacting Protein Required for ATR Signaling*. *Science*, 2011. **332**(6035): p. 1313-1317.
61. Yan, Y., et al., *Protein phosphatase 2A has an essential role in the activation of [gamma]-irradiation-induced G2/M checkpoint response*. *Oncogene*, 2010. **29**(30): p. 4317-4329.
62. HORNSTEIN, M., et al., *Protein Phosphatase and TRAIL Receptor Genes as New Candidate Tumor Genes on Chromosome 8p in Prostate Cancer*. *Cancer Genomics - Proteomics*, 2008. **5**(2): p. 123-136.

Appendix A: Hits from the phosphatome- siRNA screen

Table A1: Listing of the hits from the phosphatome screen performed prior to this thesis. Three siRNAs targeting the same gene were plated in three different 384-well plates respectively. Plate 1, 2 and denotes the three siRNA transfections. The hits were scoring with MI higher or equal to 1% H3Ser10p-positive cells.

Plate 1:(PhosA1)	% H3Ser10p-positive cells	Plate2: (PhosB1)	% H3Ser10p-positive cells	Plate 3: (PhosC1)	% H3Ser10p-positive cells
<u>DUSP16</u>	3,694	<u>PPP1CC</u>	3,852	<u>PTPRG</u>	4,082
<u>CTDSP1</u>	1,529	<u>SACM1L</u>	3,692	<u>PTPN7</u>	2,692
<u>LOC283871</u>	1,322	<u>SSH3</u>	3,439	<u>NTRK1</u>	2,469
<u>ACYP1</u>	1,309	<u>PPP4C</u>	2,477	<u>PPM2C</u>	2,365
<u>TNS</u>	1,233	<u>RAC1</u>	2,102	<u>PPP1CB</u>	1,587
<u>ACPT</u>	1,044	<u>ACP5</u>	1,711	<u>PPP2CB</u>	1,325
<u>SSH2</u>	0,943	<u>NFKBIA</u>	1,691	<u>NFKBIB</u>	1,25
<u>ACP2</u>	0,834	<u>ALPL2</u>	1,674	<u>PPP1CC</u>	1,117
		<u>SGPP2</u>	1,42	<u>PTPRN2</u>	1,099
		<u>ACPP</u>	1,205		

Appendix B: Raw- and normalized data (MI) from flow cytometry analysis

Table B1: Mitotic Indexes from Flow Cytometry of Early G2 checkpoint experiments in U2OS cells. Sorted on experiment date are shown below. Raw data and relative values are listed. Blank cells indicate that the experiment was not performed. The data is sorted by experiment date.

Early G2 Checkpoint						
	110202		110207			
	0Gy	6Gy	0Gy	6Gy		
mock	1,1	0	0,7	0		
Wee1i 100nM	1,9	0,6	2,4	0,1		
Wee1i 300nM	1,3	0,3	3,3	0,1		
Wee1i 1000nM	1,8	1,7	4,5	1,4		
Normalized to mock 0Gy	0Gy	6Gy	0Gy	6Gy		
mock	1	0	1	0		
Wee1i 100nM	1,73	0,6	3,43	0,1		
Wee1i 300nM	1,18	0,3	4,71	0,1		
Wee1i 1000nM	1,64	1,7	6,43	1,4		
	110210		110223		110303	
	0Gy	6Gy	0Gy	6Gy	0Gy	6Gy
mock	0,5	0,1	0,6	0	0,5	missing
Wee1i 100nM	1	0				
Wee1i 300nM	1	0,1	missing	1,3	2,1	0,7
Wee1i 1000nM	1,8	0,5	4,6	4,8		
normalized	0Gy	6Gy	0Gy	6Gy	0Gy	6Gy
mock	1	0,1	1	0	1	missing
Wee1i 100nM	2	0				
Wee1i 300nM	2	0,1	missing	2,17	4,2	1,4
Wee1i 1000nM	3,6	0,5	7,67	8		

Table B2: Mitotic Indexes from Flow Cytometry of Late G2 checkpoint experiments in U2OS cells. Sorted on experiment date are shown below. Raw data and relative values are listed. Blank cells indicates that the experiment was not performed The data is sorted by experiment date.

Late G2 checkpoint U2OS				
	110223		110303	
	Nocodazole	6Gy Nocodazole	Nocodazole	6Gy Nocodazole
mock	14,3	3,3	11,6	0,2
Wee1i 300nM	17,9	16,9	16,6	15,2
Wee1i 1000nM	28,6	23,3		
Values normalized to mock 0Gy				
	Nocodazole	6Gy Nocodazole	Nocodazole	6GyNocodazole
mock	1	1	1	1
Wee1i 300nM	1,25	5,12	1,43	76
Wee1i 1000nM	2	7,06		
Values normalized to Nocodazole alone:				
	Nocodazole	6Gy Nocodazole	Nocodazole	6Gy Nocodazole
mock	1	0,23	1	0,02
Wee1i 300nM	1,25	1,18	1,43	1,31
Wee1i 1000nM	2	1,63		

Table B3: Mitotic Indexes from Flow Cytometry of Early G2 checkpoint experiments in U2OS cells. Sorted on experiment date are shown below. Raw data and relative values are listed. Blank cells indicate that the experiment was not performed. The data is sorted by experiment date.

early G2 checkpoint			Cell line /experiment date		
U2OS			U2OSp53dd		
110303	0Gy	6Gy	110303	0Gy	6Gy
mock	0,5	missing		0,2	0
Wee1i 300nM	2,1	0,7		1,7	0,6
Values normalized to mock 0Gy			Values normalized to mock 0Gy		
110303	0Gy	6Gy		0Gy	6Gy
mock	1	missing		1	0
Wee1i 300nM	4,2	1,4		8,5	3
U2OS			U2OSp53dd		
110407	0Gy	6Gy	110407	0Gy	6Gy
mock	0,3	0		0,5	0
Wee1i 300 nM	1,7	1		2,7	1,1
Values normalized to mock 0Gy			Values normalized to mock 0Gy		
110407	0Gy	6Gy	110407	0Gy	6Gy
mock	1	0		1	0
Wee1i 300 nM	5,67	3,3		5,4	2,2